Atmospheric Pollution Research 12 (2021) 375–390

Contents lists available at ScienceDirect

Atmospheric Pollution Research

journal homepage: www.elsevier.com/locate/apr

Temporal and spatial variability of carbonaceous species (EC; OC; WSOC and SOA) in $PM_{2.5}$ aerosol over five sites of Indo-Gangetic Plain

Himadri S. Bhowmik [a], Shubham Naresh [a], Deepika Bhattu [d], Neeraj Rastogi [e], André S. H. Prévôt [c,**], Sachchida N. Tripathi [b,*]

[a] Department of Civil Engineering, Indian Institute of Technology Kanpur, Kanpur, Uttar Pradesh, 208016, India
[b] Department of Civil Engineering and Centre for Environmental Science and Engineering, Indian Institute of Technology Kanpur, Kanpur, Uttar Pradesh, 208016, India
[c] Laboratory of Atmospheric Chemistry, Paul Scherrer Institut, Villigen, PSI, 5232, Switzerland
[d] Department of Civil and Infrastructure Engineering, Indian Institute of Technology Jodhpur, Rajasthan, 342037, India
[e] Geosciences Division, Physical Research Laboratory, Ahmedabad, 380009, India

ARTICLE INFO

Keywords:
Carbonaceous aerosol
Elemental carbon (EC)
Organic carbon (OC)
Water soluble organic carbon (WSOC)
Secondary organic carbon (SOC)
Secondary organic aerosol (SOA)

ABSTRACT

A year-long offline based study was performed at five sites of Indo-Gangetic plain to get the spatio-temporal variation in elemental carbon (EC), organic carbon (OC), water-soluble organic carbon (WSOC) and secondary organic aerosol (SOA) in $PM_{2.5}$ fraction. OC constitutes ~70–90% of the total carbon with high water-soluble fraction (60–70%) during winter, except at Hisar. The change in concentration of OC was insignificant during summer, whereas the water-soluble fraction increased by 75–85%. The relatively high OC/EC ratio (7–11) and OC/K^+ ratio (10–52) during winter and post-monsoon suggest the dominance of biomass burning from wood fuel and agricultural waste. EC is nearly constant over the seasons at all sites suggesting the dominant presence of traffic-originated EC throughout the year. Interestingly, a low correlation (~0.3) between OC and EC at IITD and IITMD indicates their source from different origins. Exceptionally, the daytime OC/EC ratio was slightly higher than night time during winter at Hisar. However, other sites showed the opposite trend. A significant linear relationship between WSOC and secondary organic carbon suggests dominant contribution from SOA. A paired *t*-test results indicate much of WSOC is of secondary origin and regional in nature. The secondary fraction contributed 30–60% of OC during winter across all the sites in IGP, whereas during summer it varied between 20 and 40%. SOA estimated by the EC- tracer method has the highest contribution at IITMD (~138 $\mu g/m^3$) among all the sites and peaked during post-monsoon.

1. Introduction

Air pollution is a global problem which degrades the air quality (3~4-time higher $PM_{2.5}$ concentration than NAAQS), reduces visibility (IPCC, 2013), reduces crop yield, causes cardiopulmonary diseases followed by premature death (Sun et al., 2010; Viana et al., 2008; Zhang et al., 2014), and it is also responsible for altering earth's radiation balance. From degrading air quality, visibility reduction to absorb and scatter solar radiation, and altering the earth radiation balance, particulate matter can also indirectly influence the regional hydrological cycle by reducing effective cloud radius (Menon et al., 2002). Several epidemiological studies (Dockery, 2001) suggested that long term exposure to fine particulate matter ($PM_{2.5}$ ~ less than or equal to 2.5 μm in aerodynamic diameter) can reach the deepest part of lungs and causes cardiopulmonary diseases followed by myocardial infractions death. In the present-day situation, a large stretch of the Indo-Gangetic plain suffers from sequential degradation of ambient air quality and associated health issues due to emissions from several anthropogenic activities like biomass burning and waste burning, coal-fired power plant and vehicular emissions. The situation becomes worse during winter (December–February). Not only local emissions but also the long-range transport of pollutants impact the variability to the aerosol composition and also affect the rainfall pattern over India (Ram and Sarin, 2010). Carbonaceous aerosols consist of organic (OC) and elemental carbon

Peer review under responsibility of Turkish National Committee for Air Pollution Research and Control.
* Corresponding author.
** Corresponding author.
E-mail addresses: andre.prevot@psi.ch (A.S.H. Prévôt), sachchida.tripathi@gmail.com, snt@iitk.ac.in (S.N. Tripathi).

https://doi.org/10.1016/j.apr.2020.09.019
Received 30 June 2020; Received in revised form 28 August 2020; Accepted 26 September 2020
Available online 28 September 2020

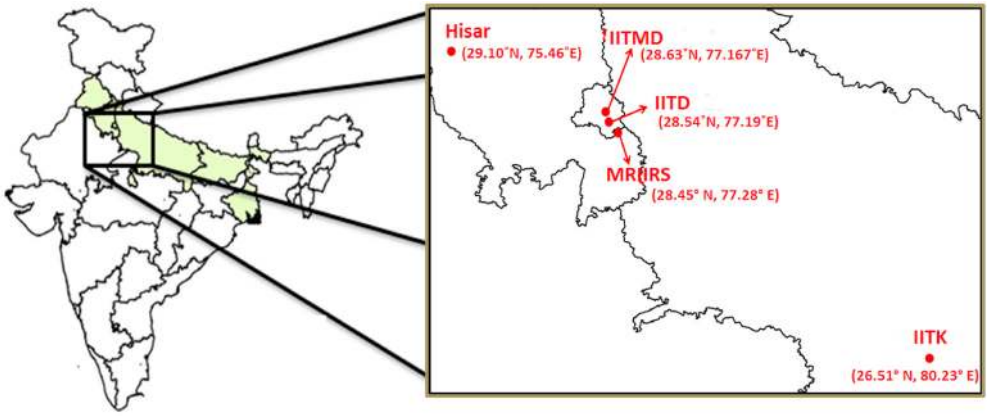

Fig. 1. Sampling sites.

(EC) and can include hundreds of organic species (Turpin and Lim, 2001), constitute up to ~10–70% of the fine particulate matter in the urban atmosphere (Chen et al., 2019; Fuzzi et al., 2006; Liu et al., 2018; Rengarajan et al., 2007; Srinivas and Sarin, 2014). Aerosols can be primary (e.g., emitted directly from the combustion process), or they can be secondary (gas to particle formation after chemical oxidation). EC is produced during the incomplete combustion of carbon-based fuels, mainly wood used for residential purposes, fossil fuel used in transportation and coal-fired power plants, etc. EC is primary in nature, and these soot particles are often associated with other chemicals attached to their surface. OC can be directly emitted in particulate form and can also be formed from gas to particle conversion (secondary) processes from the volatile organic compounds (VOCs) present in the ambient atmosphere. The amounts of OC and EC in the atmosphere and OC/EC ratios are one of the salient parameters for the evaluation of the direct or indirect impacts of aerosols on the regional scale radiative forcing (Novakov et al., 2005). The OC/EC ratios highly depend on the fuel type, quantity, and also, their combustion efficiency. OC/EC ratios can be used from offline measurements with OC-EC Carbon analyser which can also be compared with online OA/BC ratios obtained from AMS (Aerosol Mass Spectrometer). Though online study is much more accurate due to high time resolution than filter-based offline studies, we performed offline based study because of the high cost involved in the online study. There are insufficient studies on SOA in IGP, and the largest difficulty lies in the complexity of the formation process and chemical composition of SOA. SOA can be produced by both gas to particle partitioning mechanism by photo-oxidation of the VOCs (by O_3 and OH radical) and aqueous phase mechanism by scavenging of VOCs inside fog droplets. The direct estimation of SOA is way more complex due to numerous precursors (anthropogenic and biogenic) involved in its production and different formation pathways, requiring costly analytical procedure to identify and quantify. In this study, SOA has been estimated by an indirect method known as EC- tracer method. The long-term measurements of carbonaceous aerosols from IGP are limited to only a few months of data, fewer sites, and inadequate researches (e.g., Rengarajan et al., 2007; Rajput et al., 2014). Hence there is a pressing need for long-term measurements of carbonaceous aerosols over IGP.

The Indo-Gangetic Plain (IGP) which extends from 21.75°N, 74.25°E to 31.0°N, 91.5°E, is one of the most populated and heavily polluted regions in northern India. A recent study revealed 6 out of 10 most polluted cities in the world are in India, and the top listed cities like Delhi, Faridabad, Kanpur, and Lucknow are in the Indo-Gangetic plain (IGP) (World Economic Forum). IGP suffers from the enormous increase in the atmospheric concentration of air pollutants and is led by the emissions from sources like biomass and waste burning, coal-fired power plants, and vehicular emissions, etc. Further, during winter, a large part of the IGP region faces severe air pollution conditions like haze with visibility problems and even smog formation and associated health issues. To get a view of the aerosol loading in the region, information of the optical properties of fine and coarse mode aerosols are important. Sharma & Kulshrestha (2014) obtained a relatively high mean aerosol optical depth at 500 nm (AOD 500 = 0.82 ± 0.39), associated with a moderate Angstrom exponent (α) 440–870 of 0.95 ± 0.37 suggesting significant urban/industrial and biomass-burning contribution. Singh et al. (2004) and Dey et al. (2005) also have shown that in Kanpur, the average $\alpha > 1$ for 2001–2004 indicates dominance of anthropogenic aerosols during winter and post-monsoon seasons. The single scattering albedo (SSA) at 678 nm obtained in Ram et al., (2012) varied from 0.71 to 0.97 (average: 0.85 ± 0.06) during winter at Kanpur. The high absorption coefficient and low SSA during the winter at Kanpur suggested the presence of aerosols with high absorbing nature compared to those in the summer. Though some studies (Ram and Sarin, 2010; Srivastava et al., 2014; Tiwari et al., 2013) have been conducted on the chemical speciation of $PM_{2.5}$ mass at Delhi and Kanpur region, no detailed study has been carried out for intra and inter-seasonal variation as well as day-night variation in the chemical composition of $PM_{2.5}$ mass at multi-sites which covers a large part of IGP over a full-year period. Also, due to lack of measurements, issues have been faced for PM level simulations in modelling studies. Hence, understanding the main constituents and their emission sources is a prerequisite for the development of appropriate mitigation policies. In this context, our study presents a one-year data set of OC, EC, WSOC, and SOA in $PM_{2.5}$ mass from 5 different sites from upwind to downwind of IGP.

2. Methodology

2.1. Site description

The sampling campaign was carried out for a period of one full year (2018) over five sites in IGP; viz, 3 sites in National Capital Region (NCR), one in upwind direction, and other in downwind direction. The site selection was made in such a way that they align in the direction of the prevailing winds (Northwest to Southeast) at the sampling locations (see Fig. 1). High volume samplers (1.13 m^3/min) were installed to collect $PM_{2.5}$ filter samples at all five sites.

2.1.1. Hisar

The sampling was done at Agrimet Observatory (29.10°N, 75.46°E; ~215 m amsl), Department of Agricultural Meteorology, Chaudhary Charan Singh Haryana Agricultural University (CCSHAU) Hisar in the

state of Haryana. The temperature varies from 33 ± 8 °C during summer and, the winter is cold (15 ± 6 °C) with weak (<1 m/s) north-easterly winds (Rengarajan et al., 2007). It is a semi-arid sub-urban upwind site of NCR surrounded by open agricultural fields, and hence extensively impacted by biomass/crop residue burning and domestic fuel combustion emissions during crop harvesting period (April–May and Oct–Nov) and winter season, respectively (Rengarajan et al., 2007). The sampler was kept at ground level of the sampling site, located in the west direction of main city Hisar and <200 m away from less busy road.

2.1.2. Delhi-National Capital Region (NCR)

Delhi-National Capital Region (NCR) encompasses an area of 58,000 km^2, which consists of the National Capital Territory of Delhi (NCT) and some districts from adjoining states of Uttar Pradesh, Haryana, and Rajasthan with a population over 47 million. The summer is hot (20 °C–48 °C) and dry, and the winter is humid and cold (2 °C–15 °C) and dominant by the north-westerly winds during most of the year (Lalchandani et al. manuscript under review). Because of the unprecedented $PM_{2.5}$ levels, the NCR has received high attention over the world. The presence of power plants, small- and large-scale industries, mammoth increase in construction activities and other anthropogenic activities massively reduces the air quality (Rai et al. in press; Sharma and Kulshrestha, 2014). In addition, rapid increase in the vehicle numbers, from 3.3 million vehicles in 2000 to 11 million in 2018 (Economic Survey of Delhi, 2018–19) in the city, is a major concern in response to the air quality. The air quality index (AQI) remains in the worst category during the month of November. Moreover, large-scale stubble burning in Punjab and Haryana, placed in the prevalent upwind direction (North-West) of NCR, is a common practice during November.

2.1.2.1. NCR site 1: IITD. Samples were collected on the roof top of Centre for Atmospheric Science (CAS) building at Indian Institute of Technology, Delhi (28.54°N, 77.19°E; ~218m amsl) about ~15m above the ground level. It is a residential campus surrounded by hotels and restaurants and <200 m away from heavy traffic road. Recent studies from Lalchandani et al. (manuscript under review); Rai et al. (in press) showed that this site is heavily polluted with emissions from industries, power plants, vehicles and waste burning.

2.1.2.2. NCR site 2: IITMD. Sampling was conducted on the roof top of the main building at the Indian Institute of Tropical Meteorology Delhi (28.63°N, 77.167°E; ~220 m above msl) about 15 m above the ground level and is around 14 km away from another sampling site IITD. The institute is situated on the northern side of the Central Ridge reserve forest in a residential area of New Delhi (Tobler et al. manuscript under review). Lalchandani et al. (manuscript under review) showed the site is dominated by emissions from traffic, solid fuel burning and oxidized organic aerosols.

2.1.2.3. NCR site 3: MRIIRS. Sampling was carried out on the second floor of the C block building (~7m agl) at Manav Rachna International Institute of Research and Studies (MRIIRS) (28.45°N, 77.28°E ~278m above msl) which is nearly 40 km North-west to Delhi. The sampling site was an educational institute and close to main road with heavy traffic load from mainly heavy-duty trucks.

2.1.3. IITK

The downwind (~500 km of NCR region) sampling site was at the roof top of the Centre for Environmental Science and Engineering (CESE) building at Indian Institute of Technology Kanpur (26.51°N, 80.23°E ~142 m above msl) and upwind of the emission sources from the city. It is a densely populated and highly polluted sub-urban area in the IGP. The widespread impact of biomass burning emissions is noticeable, especially during winter due to the common practice of wood fuel burning for domestic use in the adjoining village Nankari and Barasirohi. The other significant sources of pollution in this locality are open burning, automobiles followed by emissions from leather industries, various small-scale industries and power plants (Tripathi et al., 2005).

2.2. Analytical Measurements

Quartz filter papers (Whatman; 8 × 12 inches) were used for collecting $PM_{2.5}$ aerosols. Daily 12 h (January to mid-March 2018) and biweekly 24 h (mid-March to December 2018) samples were collected to account for day-night and long-term variations, respectively. Field blanks were collected by loading and unloading a fresh filter in the sampler after few minutes without running the sampler. A total of 700 filters collected at five sites, including field blanks and sampled filters, were stored in the freezer section of refrigerator and periodically transferred to CESE (Centre for Environmental Science and Engineering), IIT Kanpur. Further, the samples were stored at −20 °C in the deep freezer until further analysis. The samples were analysed for elemental carbon (EC), organic carbon (OC) and total organic carbon (TOC), and major anions and cations (Na^+, K^+, Ca^{+2}, Cl^- and SO_4^{-2}) using EC-OC analyser, TOC-L analyser and Ion Chromatography, respectively. More details of analytical procedures are given below.

2.2.1. Organic Carbon (OC) and Elemental Carbon (EC)

The OC-EC analysis was carried on EC-OC carbon analyser (Model no-4F, Sunset laboratory Inc., USA) using TOT (Thermal Optical Transmittance) protocol. Field blank filters from each site were analysed, and their contribution (<0.2 μg/m^3) was removed from the respective sampled filters and errors were propagated. 1.5 cm^2 punch area of each filter was used to analyse the carbon content. Among the most commonly used protocols viz., NIOSH870 (National Institute for Occupational Safety and Health), IMPROVE_A (Interagency Monitoring of Protected Visual Environments) and EUSAAR_2 (European Supersites for Atmospheric Aerosol Research), EUSAAR_2 (Karanasiou et al., 2011) was used in this study. Thermograms, temperature difference and the difference in duration for the three protocols are shown in Fig. S1 and Table S1 (See Supplementary Material).

Briefly, in EUSAAR_2, the oven is purged stepwise in an inert mode (with helium) where the temperature is raised between 550 °C to 870 °C depending on the protocol chosen. OC being thermally unstable volatilize and it can pyrolytically convert to char and decrease the transmittance from the baseline leading to overestimation of EC while EC remains stable as it can only be volatilized at very high temperatures i.e., ~3650 °C (Peterson and Richards, 2002). A He–Ne laser and a photo detector are installed to monitor such changes and take them into account later. Further, the pyrolytically formed char and the EC get oxidized by an oxidizing medium (2% O_2 in He atmosphere) in the second phase and subsequently increase the transmittance. A 'Split Point' is defined when the laser signal returns to the baseline. The pyrolyzed carbon fraction evolved in He mode before the split point is added to OC, whereas the later fraction is termed as EC. TC was observed to be comparable among all protocols $TC_{EUSAAR\_2} = 1.1xTC_{NIOSH870}$ ($R^2 = 0.99$), $TC_{EUSAAR\_2} = 1.06xTC_{IMPROVE\_A}$ ($R^2 = 0.99$) and $TC_{IMPROVE\_A} =$

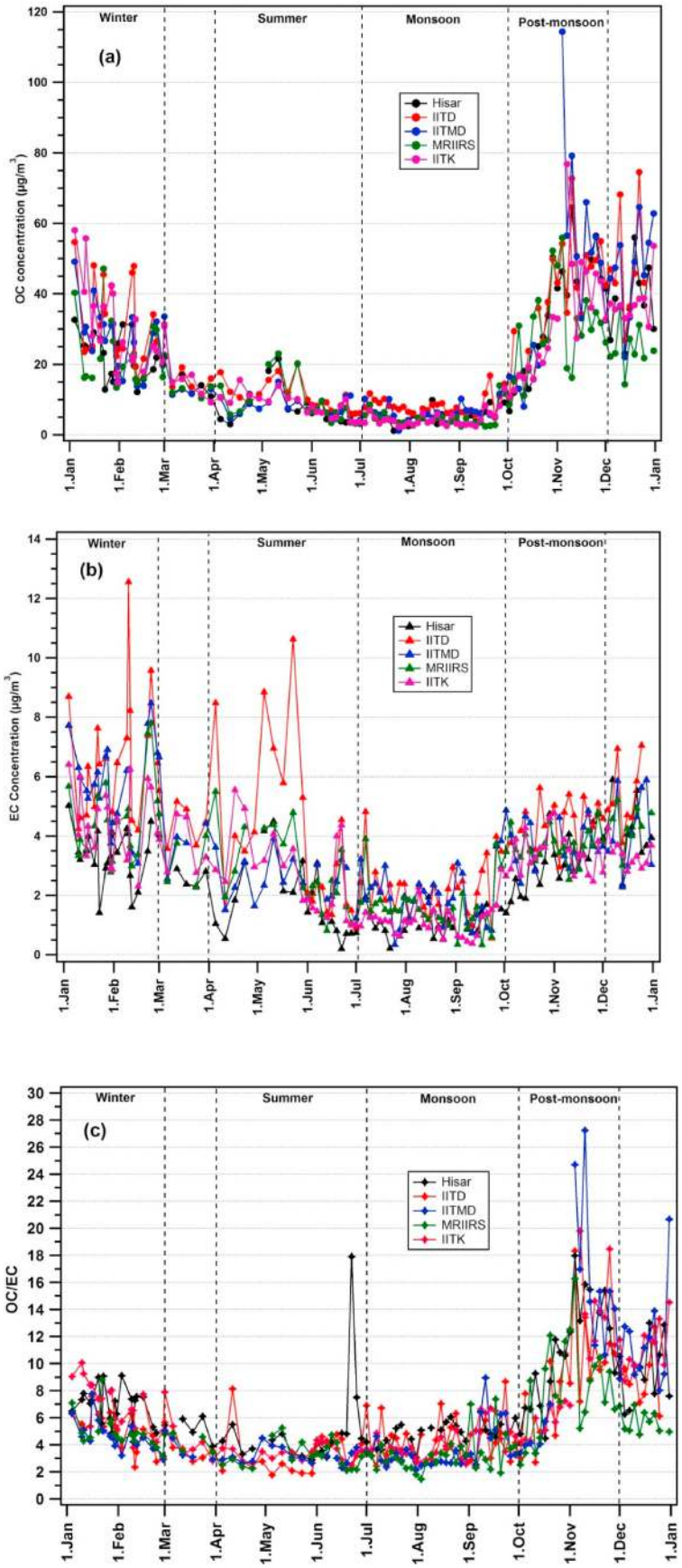

Fig. 2. Seasonal variations in (a) OC mass concentrations, (b) EC mass concentrations and (c) OC/EC ratios at the sampling sites during Jan-Dec 2018.

$1.03xTC_{NIOSH870}$ (R^2 = 0.99) (Figs. S2(b) and (c) and (d) in Supplementary Material), however OC and especially, EC concentration varied significantly. EC calculated using TOT for NIOSH870 was found to be 27% lower than for EUSAAR_2 (Fig. S2(a) in Supplementary Material). The differences can occur due to differences in the transmittance or reflectance, optical method used for the charring carbon correction, which usually results in greater EC concentrations (Chow et al., 2004; Maenhaut and Claeys, 2011). NIOSH protocol prematurely evolves EC in OC4 pure He mode, whereas IMPROVE_A protocol leads to misclassification of OC as EC2 in He/O_2 mode due to insufficiently higher temperature (580 °C). To minimize these negative and positive EC bias of NIOSH and IMPROVE A protocols (Bautista et al., 2015), EUSAAR_2 protocol has been used in this study (Panteliadis et al., 2015; Cavalli and Putaud, 2008).

2.2.2. Water-soluble organic carbon (WSOC)

For WSOC analysis, 9 cm^2 punch area of each collected filter was soaked in a 30 ml of ultrapure de-ionized water (18.2 MΩ cm) in a precleaned borosilicate test tube for ~12 h to ensure complete solubilisation of water-soluble organic carbon and inorganic ions followed by ultrasonication for 50 min and filtration using 0.2 μm quartz filter paper. As the amount of water used for extraction of WSOC can have effect on solubility, Psichoudaki and Pandis (2013) proposed a P value of $0.1 cm^3 m^{-3}$ for organic aerosol concentrations of 1–10 μg m^{-3}, where P is the ratio of water added per volume of air sampled on the analysed filter. In this study, the organic aerosol concentration ranges were on the higher side and after attempting several trials, a P value of 0.05–0.06 $cm^3 m^{-3}$ was used. Water-soluble organic carbon (WSOC) is measured for all the filtrates using a Total Organic Carbon (TOC-L) analyser (Model no- SHIMADZU-TOC-L-CPN, Shimadzu Corporation). An automatic injector takes 25 mL of water extract into the furnace, maintained at a temperature of 680 °C, where Total Carbon (TC) is oxidized to CO_2 in the presence of a catalyst (Pt). The evolved CO_2 is detected using a non-dispersive infrared (NDIR) detector after passing through a humidifier and halogen scrubber to evaluate the total carbon (TC) content. Another aliquot of the solution is acidified with HCl and the evolved CO_2 is defined as inorganic carbon (IC). The difference between TC and IC is used as a measure of WSOC in the aerosol samples. The uncertainty in WSOC relative measurement is ±5–10%. Contribution of WSOC from the blank filters was removed from the sampled filters. The detection of TC and IC by NDIR detector is calibrated using the standard solutions of potassium hydrogen phthalate and sodium carbonate-bicarbonate mixture (Na_2CO_3+$NaHCO_3$; 1:1 vol/vol), respectively. Triplicates of TC and IC were generated to achieve a coefficient of variation (CV) less than 2%.

2.2.3. Water soluble inorganic ions

The same filtrate (similar to that used for the analysis of WSOC) of the extracted filters was used for Na^+, K^+, Ca^{+2}, Cl^- and SO_4^{-2} by an Ion chromatograph (Metrohm 883 Basic IC plus for cations and 882 compact IC plus for anions). The instrument was equipped with two separate columns for the analysis of cations and anions. An AS 5–250/4.0 chromatography column was used to separate the anions with 3.2 mM Na_2CO_3+1 mM $NaHCO_3$ solution as an eluent along with the anion self-regenerating suppressor. For cations, C-6 column was used with 2.7 mM HNO_3 solution as an eluent, along with the cation self-regenerating suppressor, which is connected in series. The injected sample carried by the mobile phase (eluents) passes through the columns equipped with a charged stationary phase for separating the ions depending on their polarity. The range of calibration standards was prepared using appropriate dilutions of the stock. The coefficient of variation (CV) calculated from repeat samples was 1.4%.

3. Results and Discussions

The spatiotemporal variation in the aerosol mass concentration and its chemical composition highly depends on regional meteorology, topographical features and emission sources. Indo-Gangetic Plain (IGP) extends from northeast to northwest and parallel to the Himalayan range. This flat topography, along with shallow boundary layer height and moderate winds during winter, favors confining of the aerosols in the atmosphere. Delhi NCT being upwind part of the IGP is one of the highly polluted regions in the world (Pant et al., 2015; Tiwari et al., 2013). Also, recent study by Chowdhury et al. (2019) examined the build-up of $PM_{2.5}$ over Delhi NCR based on 16 years (2001–2016) of high-resolution MODIS MAIAC 1 km satellite data and validated against the CPCB monitoring stations. This has led to the IGP being recognized as one of the most important hotspots in India as well as in South Asia for aerosol production (Joshi et al., 2016; Rengarajan et al., 2007). The southwest monsoon brings the season's monsoon during July to September and responsible for 70–80% of the annual precipitation. In summer, the desert dust from North Western India, while mixing with the locally generated BC, forms a rigorously absorbing mixture that absorbs incoming solar radiation and rise up through the lower troposphere to accumulate along the southern slopes of the Himalayas (Ram and Sarin, 2010; Sharma and Kulshrestha, 2014). The temporal variability in the aerosol composition has been discussed in terms of four different seasons as winter (December–February), summer (April–June), monsoon (July–September), and post-monsoon (October–November) as described by Indian Meteorological Department (IMD). March is the transition phase between winter and summer. Generally, the major wind regime during the winter was north-westerly, and occasionally from the northeast and southwest during summer. Though several small-scale field campaigns had been conducted in the past, to investigate the physicochemical and optical properties of the ambient aerosols over few hotspots in IGP (Nair et al., 2007; Ram and Sarin, 2010; Sharma and Kulshrestha, 2014), no multi-site long-term field campaign has been conducted in the past covering a large stretch over IGP. To the best of our knowledge, this is the first multi-site (5) yearlong comprehensive study investigating the temporal variations in carbonaceous aerosols over IGP and estimating the primary and secondary organic carbon fraction.

3.1. Mass concentration of EC, OC and OC/EC ratios

A large temporal and spatial variability in EC and OC concentrations was observed during the sampling period (January 2018 ~ December 2018) with the mass concentrations of OC varied annually from 1.2 to 64.6 μg/m^3 at Hisar, 4.9–74.6 μg/m^3 at IITD, 1.2–114.4 μg/m^3 at IITMD, 2.4–55.9 μg/m^3 at MRIIRS, and 2.4–76.9 μg/m^3 at IIK. Similarly, the EC concentrations varied annually from 0.2 to 5.9 μg/m^3 at Hisar, 0.6–12.6 μg/m^3 at IITD, 0.3–8.5 μg/m^3 at IITMD, 0.3–7.8 μg/m^3 at MRIIRS and 0.4–6.4 μg/m^3 at IITK. The average seasonal and the day-night (Jan–Feb) mass concentrations of EC and OC at these 5 sites are presented in Table 2.

Overall, the average OC concentrations during winter and post-monsoon were 3–4 times higher than summer at all the sites. OC and EC were higher during post-monsoon, followed by winter, summer and

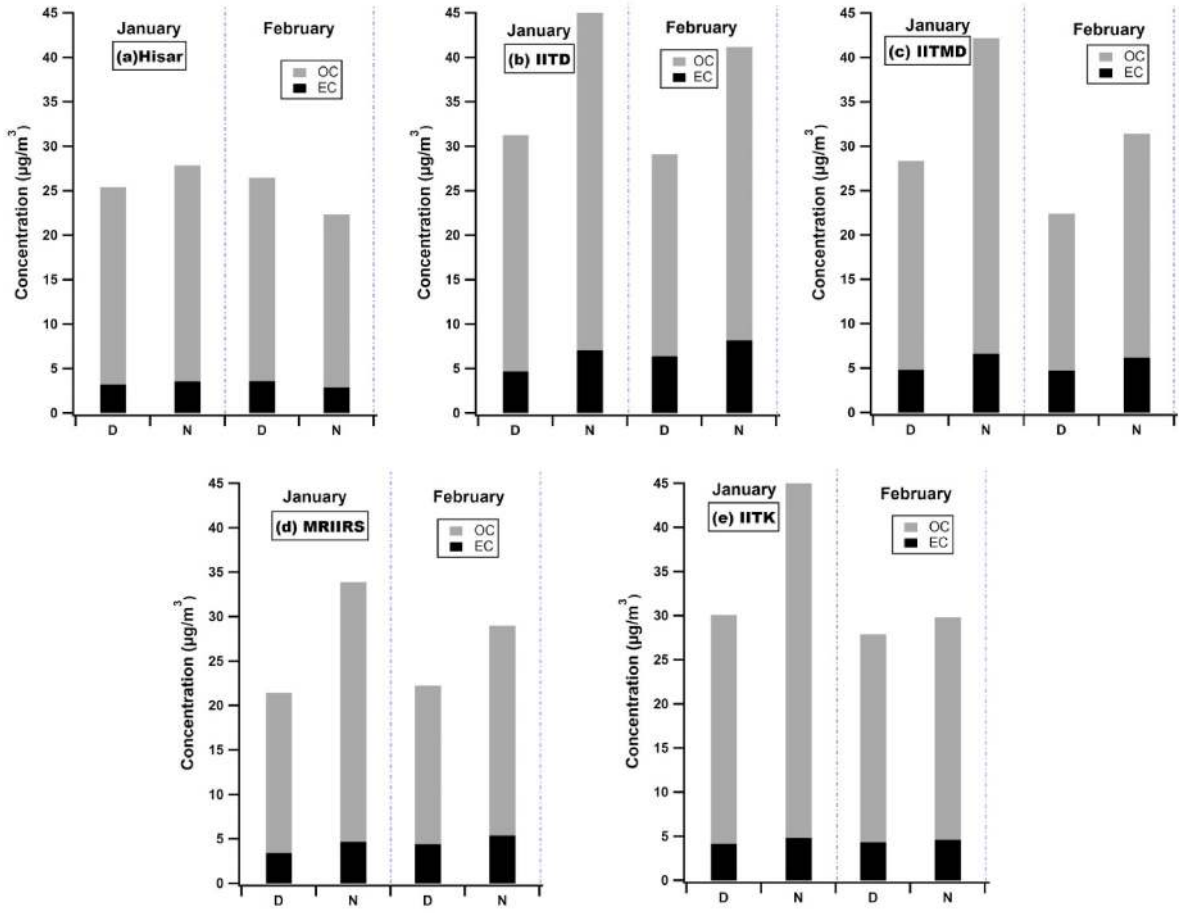

Fig. 3. Day-Night average concentration of EC and OC during Jan-Feb 2018 at the sampling sites.

monsoon at all the sites (See Fig. 2). The main factors causing a high mass concentration of OC and EC were lower planetary boundary layer height along with increase in the source strength during post-monsoon and winter. IITMD is the most polluted site amongst others with OC concentrations varying from 42.2 ± 28.8 μg/m^3 during post-monsoon, 27.3 ± 9.2 μg/m^3 in winter, 8.4 ± 2.8 μg/m^3 in summer and 6.3 ± 2.6 μg/m^3 in monsoon followed by IITD, Hisar, IITK and MRIIRS. The OC concentrations in IITD varied from 40.12 ± 15.5 μg/m^3 during post-monsoon, 31.5 ± 11.7 μg/m^3 in winter, 10.9 ± 3.9 μg/m^3 in summer and 8.4 ± 2.6 μg/m^3 in monsoon. In Hisar, the OC concentrations were 34.4 ± 16.9 μg/m^3 during post-monsoon, 22.6 ± 6.1 μg/m^3 in winter, 7.6 ± 5.0 μg/m^3 in summer and 5.01 ± 2.3 μg/m^3 in monsoon. In IITK, the OC concentration was almost same during post-monsoon and winter and varied from 30.9 ± 12.3 μg/m^3 in winter, 30.5 ± 16.4 μg/m^3 in post-monsoon, 8.6 ± 3.2 μg/m^3 in summer and 4.6 ± 2.3 μg/m^3 in monsoon. MRIIRS is the least polluted site having OC concentrations 29.8 ± 12.9 μg/m^3 during post-monsoon, 22.8 ± 9.4 μg/m^3 in winter, 9.3 ± 5.7 μg/m^3 in summer and 4.7 ± 1.5 μg/m^3 in monsoon. Whereas IITD being closest to the heavy traffic road (<200 m away), had the highest EC concentrations amongst all sites in all seasons with values ranging from 6.5 ± 2.1 μg/m^3 during winter, 4.2 ± 2.8 μg/m^3 in summer, 4.2 ± 0.8 μg/m^3 in post-monsoon, and 2.2 ± 0.9 μg/m^3 in monsoon. The EC concentrations were the highest in winter followed by post-monsoon, summer and monsoon in all the sites except IITD having higher concentration during summer than post-monsoon. At IITMD, the EC concentrations varied from 5.8 ± 1.4 μg/m^3 in winter, 3.7 ± 0.8 μg/m^3 in post-monsoon, 2.6 ± 0.7 μg/m^3 in summer and 1.9 ± 0.8 μg/m^3 in monsoon. The seasonal EC variations in MRIIRS and IITK were almost similar. The EC concentrations in MRIIRS varied from 4.6 ± 1.4 μg/m^3 in winter, 3.7 ± 0.5 μg/m^3 in winter, 2.9 ± 1.3 μg/m^3 in summer and 1.6 ± 0.7 μg/m^3 in monsoon, whereas in IITK the EC concentrations were 4.4 ± 1.2 μg/m^3 in winter, 3.4 ± 0.6 μg/m^3 in post-monsoon, 2.8 ± 1.3 μg/m^3 in summer and 1.1 ± 0.5 μg/m^3 in monsoon. Hisar being surrounded by open agricultural field, the EC concentrations were least amongst all sites. The EC concentration varied from 3.4 ± 0.9 μg/m^3 in winter, 3.1 ± 0.9 μg/m^3 in post-monsoon, 1.9 ± 1.2 μg/m^3 in summer and 1.1 ± 0.4 μg/m^3 in monsoon. The highest OC concentration at IITD was observed during December (74.6 μg/m^3), whereas the highest peak at IITMD (114.4 μg/m^3 during Nov) and MRIIRS (55.9 μg/m^3 during Nov) was observed during Diwali. Hisar (64.6 μg/m^3) and IITK (76.87 μg/m^3) got

Table 1
Comparison of average concentrations of OC, EC and OC/EC ratios from different urban locations in developing countries.

Location	Area	Sampling Period	Size	OC (μg/m^3)	EC (μg/m^3)	OC/EC
Hisar[a]	Urban	January-December 2018	$PM_{2.5}$	18.9 ± 15.5	2.5 ± 1.4	7 ± 3.4
Delhi[a]	Urban	January-December 2018	$PM_{2.5}$	23.9 ± 17.8	4.2 ± 2.2	5.9 ± 3.4
Rajendranagar[a]	Urban	January-December 2018	$PM_{2.5}$	21.6 ± 20.4	3.5 ± 1.8	5.9 ± 4.8
Faridabad[a]	Urban	January-December 2018	$PM_{2.5}$	16 ± 12.5	3.1 ± 1.5	4.8 ± 2.6
Kanpur[a]	Urban	January-December 2018	$PM_{2.5}$	18.9 ± 15.8	2.8 ± 1.5	6.2 ± 3.6
Hisar[b]	Urban	December 2004	TSP	33.0 ± 17.9	3.8 ± 1.4	8.5 ± 2.2
Delhi[c]	Urban	January-December 2010	PM_{10}	26.7 ± 9.2	6.1 ± 3.9	4.38 ± 2.36
Kanpur[d]	Urban	January-March 2007	TSP	25 ± 13.8	4.8 ± 3	6.2 ± 3.7
Dhaka, Bangladesh[e]	Urban	March-April 2001	TSP	45.7	22	2.08
Karachi, Pakistan[f]	Urban	February 2015–March 2017	TSP	39.9 ± 22.8	8.52 ± 4.79	4.2 ± 2.5
Kathmandu, Nepal[f]	Urban	April 2013–January 2016	TSP	34.8 ± 27.1	9.97 ± 5.84	3.5 ± 2.1
Lanzhou, China[f]	Urban	December 2015–November 2016	TSP	25.4 ± 13.0	6.7 ± 3.52	3.6 ± 2.3
Beizing, China[g]	Urban	December 2016–November2017	TSP	11 ± 10.7	3.4 ± 3.3	3.7 ± 2.4
Beizing, China[h]	Urban	May-June 2016	$PM_{2.5}$	11 ± 3.7	1.8 ± 1	4.1 ± 2.6
Sao Paulo, Brazil[i]	Urban	September-November 2013	$PM_{2.5}$	2.7 ± 1.1	1.5 ± 0.7	1.8 ± 0.6
Sao Paulo, Brazil[j]	Urban	January-September 2014	$PM_{2.5}$	6.7 ± 4.4	4.1 ± 3.5	1.7 ± 0.5

[a] This study.
[b] Rengarajan et al., (2007).
[c] Sharma et al.,2014.
[d] Ram and Sarin (2010).
[e] Salam et al.,2003.
[f] Chen et al., (2019).
[g] Ji et al., (2019).
[h] Tang et al., (2018).
[i] Monteiro dosSantos et al. 2016.
[j] MartinsPereira et al. 2017.

the highest peaks during November which is the peak time for agricultural waste burning, whereas the highest EC concentration (5.9 μg/m^3 at Hisar, 12.6 μg/m^3 at IITD, 8.5 μg/m^3 at IITMD, 7.8 μg/m^3 at MRIIRS, and 6.4 μg/m^3 at IITK) was observed during mid-February at all these five sites. Again, night-time EC and OC concentrations were statistically higher (p-value< 0.05) than daytime at all sites, except at Hisar and IITK (Fig. 3). IGP is highly polluted with carbonaceous aerosols, unlike other developing countries such as Beijing of China and Sao Paulo of Brazil. A study by Monteiro dos Santos et al. (2016) conducted in Sao Paulo, Brazil during Sept to Nov 2013 observed an average OC concentration of ~2.7–3.4 μg/m^3 and an average EC concentration of ~1.5–2.3 μg/m^3 except at one site where the EC concentration is higher ~ 6.1 μg/m^3. The OC and EC mass concentrations during Sept–Nov are ~10–11 times and ~1.5–2 times lower respectively than what we observed in this study. Again the observed OC and EC mass concentrations during summer (May-June 2016) in Beijing conducted by Tang et al. (2018) were ~9–11 μg/m^3 and ~0.7–1.8 μg/m^3 respectively which is similar to the OC concentrations and ~1.4–2 times lower than the EC concentrations during May–June observed in this study.

The OC/EC ratios varied annually from 2.9 to 15.4 at upwind (Hisar), 1.7 to 13.7 at Delhi NCR and, 2.1 to 14.5 at downwind (IITK). In IITMD the OC/EC ratios varied from 11.4 ± 7.5 during post-monsoon, 4.7 ± 1.1 in winter, 3.2 ± 0.6 in summer and 3.6 ± 1.5 in monsoon. The OC/EC ratios at Hisar were found to be 10.9 ± 3.9 in post-monsoon and 6.9 ± 1.4 in winter, suggesting emissions from crop residue burning and open biomass burning during post-monsoon and winter respectively (Rengarajan et al., 2007). The ratios were 5.0 ± 3.4 in summer and 4.9 ± 0.8 in monsoon. At IITD, the ratios range from 9.8 ± 3.9 during post-monsoon, 4.9 ± 1.4 in winter, 3.3 ± 1.5 in summer and 4.3 ± 1.6 in monsoon. The OC/EC ratios at IITK varied from 9.1 ± 4.9 during post-monsoon, 6.9 ± 1.7 in winter, 3.3 ± 0.6 in summer and 4.2 ± 1.2 in monsoon. The high values in winter at IITK suggests emissions from wood-burning for domestic purpose (Ram et al., 2010). In MRIIRS the ratios were 8.2 ± 3.5 during post-monsoon, 4.9 ± 1.2 in winter, 3.2 ±

Table 2
Seasonal average and day and night average concentration (during Jan-Feb 2018) of OC, EC and OC/EC at sampling sites.

Seasons	Hisar			IITD			IITMD			MRIIRS			IITK		
	OC (μg/m^3)	EC (μg/m^3)	OC/EC	OC (μg/m^3)	EC (μg/m^3)	OC/EC	OC(μg/m^3)	EC (μg/m^3)	OC/EC	OC (μg/m^3)	EC (μg/m^3)	OC/EC	OC (μg/m^3)	EC (μg/m^3)	OC/EC
$Winter_{(Day)}$	22.4 ± 5.8	3.4 ± 0.8	6.7 ± 1.4	24.9 ± 8.7	5.5 ± 3.1	5.2 ± 1.7	20.9 ± 9.2	4.8 ± 1.4	4.3 ± 1.5	17.9 ± 4.2	3.9 ± 1.5	4.8 ± 0.9	24.9 ± 6.7	4.3 ± 1.2	6.1 ± 1.3
$Winter_{(Night)}$	22.3 ± 9.0	3.3 ± 1.3	6.8 ± 1.4	38.1 ± 18.8	7.6 ± 2.3	4.9 ± 1.6	31.6 ± 2.8	6.5 ± 0.7	4.8 ± 1.6	26.9 ± 13.4	5.0 ± 1.5	5.3 ± 1.9	36.3 ± 18.9	4.7 ± 1.5	7.6 ± 2.6
Winter	22.6 ± 6.1	3.4 ± 0.9	6.9 ± 1.34	31.5 ± 11.7	6.5 ± 2.1	5 ± 1.4	27.3 ± 9.2	5.8 ± 1.4	4.7 ± 1.1	22.8 ± 9.4	4.6 ± 1.4	5 ± 1.2	30.9 ± 12.3	4.4 ± 1.2	7 ± 1.7
Summer	7.6 ± 5.0	1.9 ± 1.2	5.0 ± 3.4	10.9 ± 3.9	4.2 ± 2.8	3.3 ± 1.5	8.4 ± 2.8	2.6 ± 0.7	3.2 ± 0.6	9.3 ± 5.7	2.9 ± 1.3	3.2 ± 0.9	8.6 ± 3.2	2.8 ± 1.3	3.3 ± 0.6
Monsoon	5.1 ± 2.3	1.1 ± 0.4	4.9 ± 0.8	8.4 ± 2.6	2.2 ± 0.9	4.3 ± 1.6	6.3 ± 2.6	1.9 ± 0.8	3.6 ± 1.5	4.7 ± 1.5	1.6 ± 0.7	3.3 ± 1.3	4.6 ± 2.3	1.1 ± 0.5	4.2 ± 1.2
Post-monsoon	34.4 ± 16.9	3.1 ± 0.9	10.9 ± 3.9	40.1 ± 15.5	4.2 ± 0.8	9.8 ± 3.9	42.2 ± 28.8	3.7 ± 0.8	11.4 ± 7.5	29.8 ± 12.9	3.7 ± 0.5	8.2 ± 3.5	30.5 ± 16.4	3.4 ± 0.6	9.1 ± 4.9

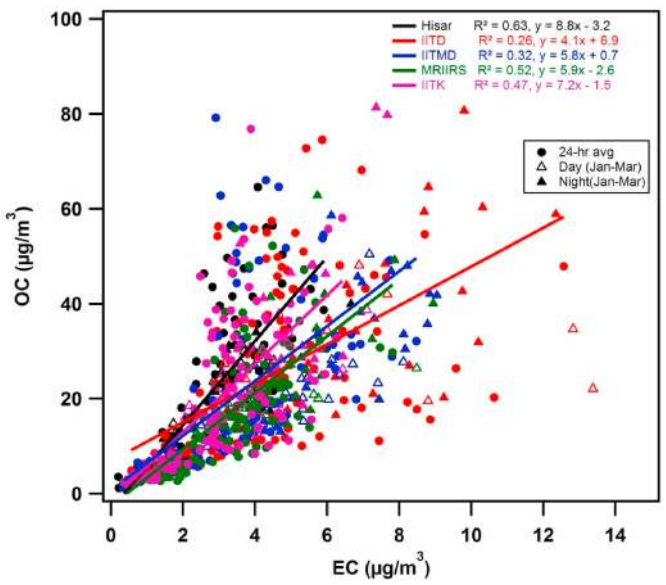

Fig. 4. Scatter plot between OC and EC at the sampling sites during Jan-Dec 2018.

0.9 in summer and 3.3 ± 1.3 in monsoon. A similar value of 6.9 ± 1.4 and 6.9 ± 1.7 was obtained at Hisar and IITK respectively during winter and attributed to the local anthropogenic emissions from fossil fuel and domestic combustion (Mikhailov et al., 2017), indicating dominance of open biomass burning at Hisar and wood-burning at IITK during winter as wood-burning from domestic purpose is a common practice in the densely populated adjoining village Nankari and Barasirohi near IITK. Average OC/EC ratios in summer (ranges from: 3.17 to 5.01) were 2.2–3.5 times lower than those in the winter and post-monsoon (ranges from: 8.17 to 11.37) at all the sites. The monthly variation in OC/EC ratios was similar at all the sites with the highest peaks observed during Nov and lowest during April–May (See Table S2 in Supplementary Material). In this study, the OC/EC ratios at all the sites during Sept–Nov suggest emission from biomass burning (~6.8–10.2), unlike the dominant contribution of emissions from light and heavy-duty vehicles (~0.56–1.88) at Sao Paulo, Brazil during Sept-Nov 2013 (Monteiro dos Santos et al., 2016). Relatively high ratios for biomass burning emissions and lower ratios for vehicular emissions (e.g.,Andreae and Merlet, 2001; Ram et al., 2010; Sandradewi et al., 2008) have been reported in many studies. A comparison of the average concentrations of OC, EC and OC/EC ratios measured over different urban locations in the developing countries (e.g., India, China, Brazil, Pakistan, Bangladesh, etc.) are shown in Table 1.

Average night-time OC/EC ratios were slightly higher at downwind site (7.57 at IITK, 5.29 at MRIIRS) compared to daytime values (6.05 at IITK, 4.83 at MRIIRS), whereas opposite trend is observed at IITD site. The lower planetary boundary layer height with weaker wind speed (<2–3 m/s) during winter nights along with active open biomass burning is likely the main reason (Rengarajan et al., 2007; Ram and Sarin, 2010) for higher OC/EC ratios at these sites. However, no statistically significant differences (p value > 0.05) were observed at upwind site. The seasonal and day-night (during Jan–Feb) average OC/EC ratios for these five sites are tabulated in Table 2.

A temporal shift in the emission characteristics and/or changes in the type of biomass burning along with meteorological factors could be responsible for the spatial and temporal variation in OC/EC ratios (Hopkins et al., 2007). However, filter sampling artifacts such as evaporation of semi-volatile species can also lead to underestimation of OC concentration and hence lower OC/EC ratios (Viana et al., 2006). Assuming this SVOC evaporation artifact is negligible; the low OC/EC ratio in summer indicates that secondary organic aerosol might not be the main driver of the OC/EC ratio but rather the biomass burning fraction in different seasons.

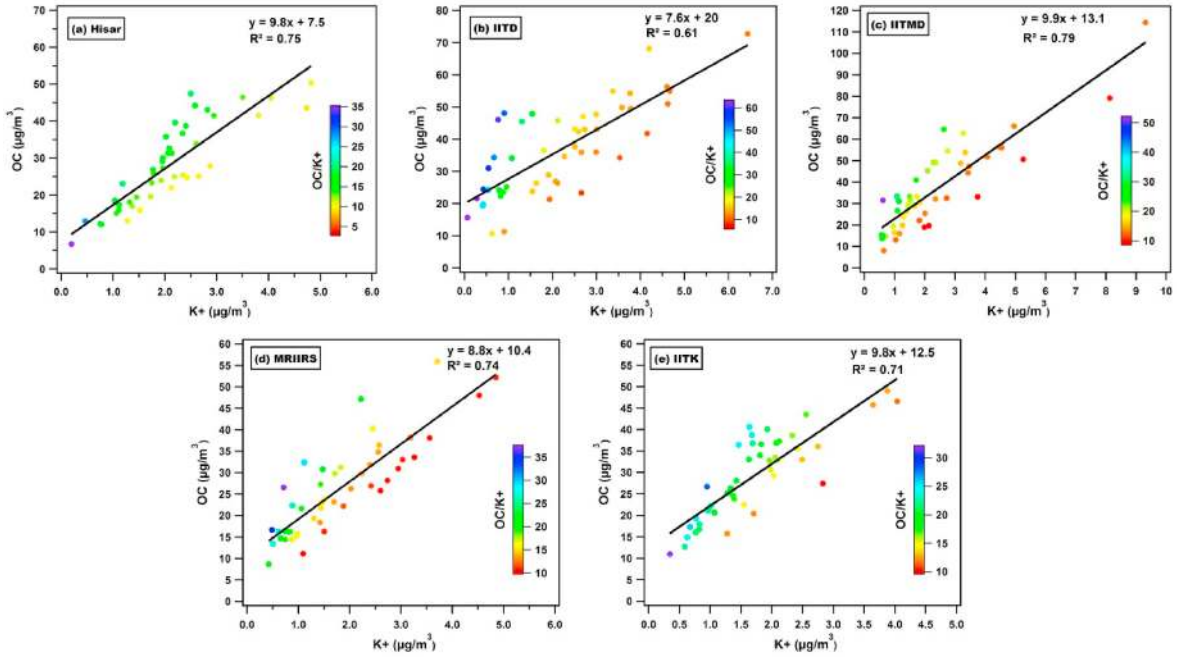

Fig. 5. Scatter plots between OC and K^+ at the sampling sites with corresponding OC/K^+ ratios during winter and post-monsoon.

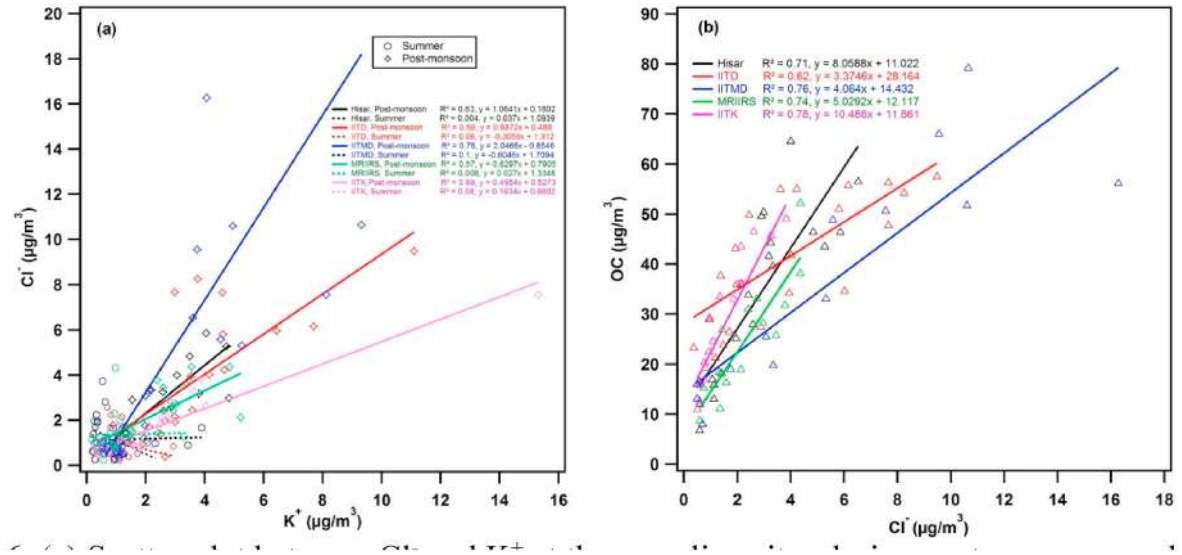

Fig. 6. (a) Scatter plot between Cl^- and K^+ at the sampling sites during post-monsoon and summer; (b) Scatter plot between Cl^- and OC at the sampling sites during post-monsoon.

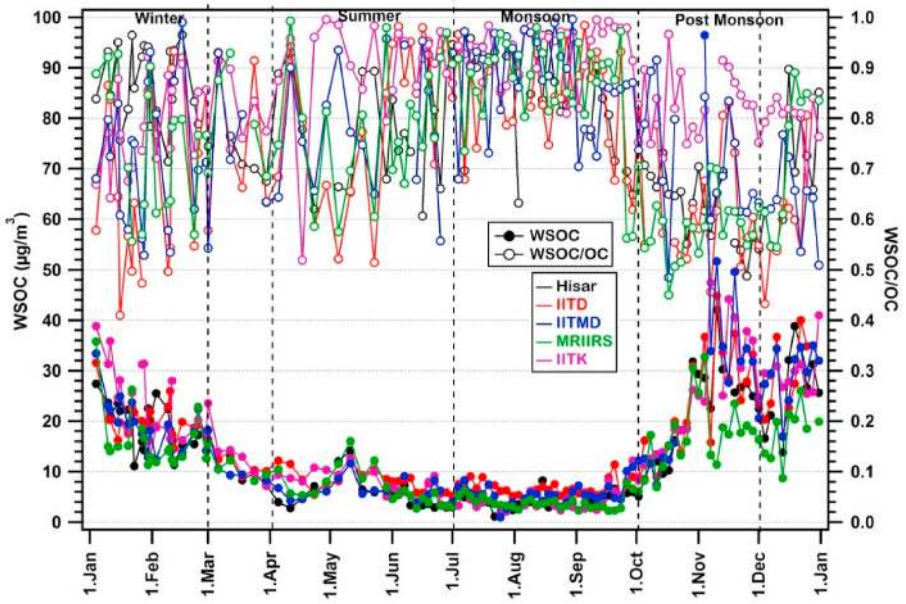

Fig. 7. Seasonal variations of WSOC and WSOC/OC in sampling sites during Jan-Dec 2018.

OC was found to be ~7–9 times of EC in upwind and downwind, whereas at NCR sites, it was ~3–6. The similarity in the slopes of linear fit between OC and EC (Fig. 4) at the sites ~ Hisar, MRIIRS and IITK suggest their origin from same sources except at IITD and IITMD. Also, a positive linear relation between OC and EC at Hisar ($R^2 = 0.63$), MRIIRS ($R^2 = 0.52$) and IITK ($R^2 = 0.47$) suggests their emissions from a common source and/or influenced by the same meteorological factors however at IITD ($R^2 = 0.26$) and IITMD ($R^2 = 0.32$) these emissions are from different sources (Fig. 4).

3.2. Source characterization by K^+ and OC/K^+ ratio

Water-soluble potassium (K^+) ion can be served as a tracer to apportion biomass burning contributions (Ramadan et al., 2000). However, during summer (April–June), in the absence of a biomass burning source, the contribution from mineral dust can be expected more due to the long-range transport from arid regions. As K^+ can have other sources (e.g., sea salt and soil dust) apart from biomass burning (Duvall et al., 2008), non-sea salt K^+ (C. A. Pio et al., 2008) contributions were calculated for this study. During summer and monsoon, the average K^+ concentration was relatively low (0.29–0.86 µg/m^3) compared to that in winter and post-monsoon (2.5–3.5 µg/m^3) at all the sites. Considering K^+/Na^+ molar ratio of 0.022 in seawater (Keene et al., 1986) and based on the annual average Na^+ concentrations, the contribution of K^+ from sea salt is negligible at all the sites (Hisar~0.01 µg/m^3, IITD~0.02 µg/m^3, IITMD~0.02 µg/m^3, MRIIRS~0.028 µg/m^3,

Table 3
Seasonal average and day and night average concentration (during Jan-Feb 2018) of WSOC and WSOC/OC at sampling sites.

Seasons	Hisar		IITD		IITMD		MRIIRS		IITK	
	WSOC (μg/m^3)	WSOC/OC	WSOC (μg/m^3)	WSOC/OC	WSOC (μg/m^3)	WSOC/OC	WSOC (μg/m^3)	WSOC/OC	WSOC (μg/m^3)	WSOC/OC
Winter$_{(Day)}$	20.5 ± 4.3	0.9 ± 0.1	18.9 ± 4.2	0.8 ± 0.2	17.6 ± 6.5	0.8 ± 0.2	14.8 ± 3.2	0.8 ± 0.1	22.4 ± 5.3	0.9 ± 0.1
Winter$_{(Night)}$	18.7 ± 5.7	0.9 ± 0.7	21.3 ± 5.4	0.6 ± 0.2	19.2 ± 6.4	0.7 ± 0.2	17.3 ± 7.3	0.7 ± 0.14	25.1 ± 9.7	0.7 ± 0.1
Winter	19.4 ± 4.6	0.9 ± 0.1	20.3 ± 3.7	0.7 ± 0.2	18.9 ± 5.2	0.7 ± 0.1	16.4 ± 6.1	0.7 ± 0.1	23.6 ± 7.6	0.8 ± 0.1
Summer	5.6 ± 3.1	0.8 ± 0.1	8.4 ± 2.1	0.8 ± 0.2	6.5 ± 2.1	0.8 ± 0.1	6.8 ± 3.4	0.8 ± 0.1	7.6 ± 2.7	0.9 ± 0.1
Monsoon	4.1 ± 1.5	0.8 ± 0.1	6.8 ± 1.5	0.8 ± 0.1	5.4 ± 2.0	0.8 ± 0.1	3.9 ± 1.3	0.8 ± 0.1	4.3 ± 2.2	0.9 ± 0.1
Post-monsoon	21.0 ± 9.8	0.6 ± 0.1	25.5 ± 9.9	0.6 ± 0.1	29.8 ± 22.5	0.7 ± 0.1	17.1 ± 7.1	0.6 ± 0.1	24.6 ± 11.8	0.8 ± 0.1

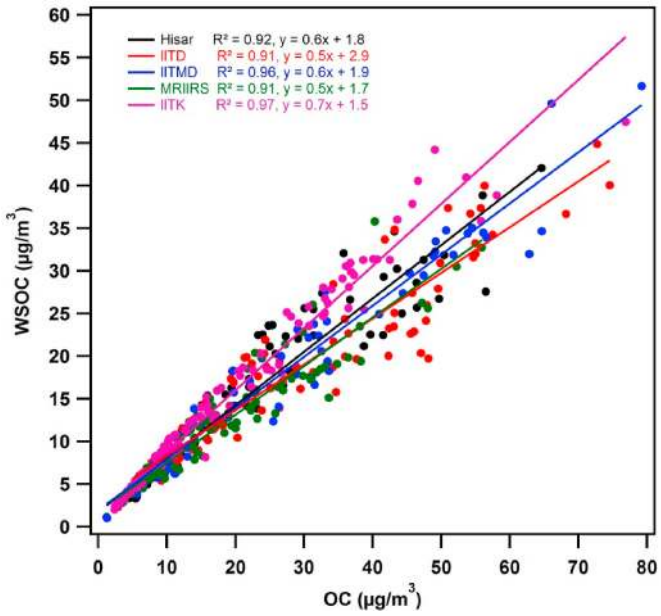

Fig. 8. Scatter plot between WSOC and OC at the sampling sites during Jan-Dec 2018

IITK~0.02 μg/m^3). A strong correlation (R^2 = 0.61–0.79) was observed between OC and K^+ in the samples collected during winter and post-monsoon at all the sites (Fig. 5). This might suggest that both K^+ and OC are strongly influenced by a common source (biomass burning). Moreover, the higher intercepts at these sites suggest influence of a background SOA contribution and/or presence of a different primary source (fossil fuel combustion). In contrast, K^+ and EC concentrations showed a large scatter (R^2 = 0.01–0.21), suggesting different dominant sources of K^+ and EC (see Fig. S3 in Supplementary Material).

A high OC/K^+ value of 10–12 and 12–25 have been suggested for savanna burning and agricultural waste burning, respectively (Andreae and Merlet, 2001). Ram and Sarin (2010) observed a value of ~16.7 (varying from 11 to 50) for Kanpur, which is well matching with our observed values at Kanpur (avg~19.18 during post-monsoon). Also, K^+ showed a similar trend as the OC/EC ratio at all the sites (see Fig. S4 in Supplementary Material).

The seasonal Cl^-/Na^+ ratios (4.28, 2.17, 2.76, 5.27 for winter, summer, monsoon, and post-monsoon respectively at Hisar; 4.02, 1.83, 2.24, 6.12 for winter, summer, monsoon, and post-monsoon respectively at IITD; 2.59, 2.13, 2.43, 3.81 for winter, summer, monsoon, and post-monsoon respectively at IITMD; 2.08, 1.14, 1.93, 2.92 for winter, summer, monsoon, and post-monsoon respectively at MRIIRS and, 4.52, 0.88, 2.18, 3.12 for winter, summer, monsoon, and post-monsoon respectively at IITK) in $PM_{2.5}$ at all the sites were larger than the typical Cl^-/Na^+ equivalent ratio (1.17) of seawater (Chester, 1990), except during summer at MRIIRS and IITK. The elevated Cl^-/Na^+ ratio (>1.17) indicated the attribution to the non-sea salt sources, such as biomass burning (Yao et al., 2002). The biomass burning derived K^+ may exist in the atmosphere greatly as KCl (Pósfai et al., 2004). The linear relationship between K^+ and Cl^- varied with strong correlation in post-monsoon (R^2 = 0.6–0.9) and weaker in summer (R^2 = 0.004–0.1) at all the sites (Fig. 6(a)) indicating K^+ existed as KCl at lower temperature in post-monsoon and higher temperature in summer may not favour the presence of KCl, but it may exist in some other chemical form such as K_2SO_4 (Zhang et al., 2013). Moreover, a good correlation between OC and Cl^- (R^2 = 0.71 at Hisar, R^2 = 0.62 at IITD, R^2 = 0.76 at IITMD, R^2 = 0.74 at MRIIRS and R^2 = 0.78 at IITK) during post-monsoon suggests their emission from a common source (biomass burning) (Fig. 6(b)).

Further, nss-SO_4^{-2}/EC can also be used as a proxy for identifying the emissions from biomass burning and fossil fuel combustion. Assuming Na^+ as a reference element, non-sea-salt fraction of SO_4^{-2} can be defined by,

$$\left[nns - SO_4^{-2}\right] = \left[SO_4^{-2}\right] - 0.125x[Na^+]$$

where the concentrations are in μeq/l. The factor 0.125 was taken for the equivalent concentration ratio of SO_4^{-2} to Na^+ in seawater (Tiwari et al., 2005).

The nss-SO_4^{-2}/EC ratios are lower in case of emissions from biomass burning compared to fossil fuel combustion (Mkoma et al., 2013). Andreae and Merlet, 2001 suggested a value of 0.7 ± 0.1 for biofuel. During the study period the nss-SO_4^{-2}/EC ratios in Hisar varied from 0.6

Table 4
Primary OC/EC ratio and R^2 for linear regression on the portion of seasonal data over the sampling sites.

Seasons	Hisar		IITD		IITMD		MRIIRS		IITK	
	$[OC/EC]_p$	R^2	$[OC/EC]_p$	R^2	$[OC/EC]_p$	R^2	$[OC/EC]_p$	R^2	$[OC/EC]_p$	R^2
Winter	3.49	0.53	2.713	0.32	3.46	0.44	2.7	0.54	3.27	0.48
Summer	2.09	0.77	1.716	0.76	2.53	0.87	2.16	0.65	2.22	0.79
Monsoon	1.8	0.62	1.64	0.65	2.1	0.83	1.73	0.64	1.9	0.73
Post-monsoon	3.63	0.60	3.48	0.28	3.57	0.25	3.09	0.43	3.72	0.39

Table 5
Seasonal average concentration of SOC, SOA and SOC/OC at sampling sites.

Seasons	Hisar			IITD			IITMD			MRIIRS			IITK		
	SOC (μg/m^3)	SOA (μg/m^3)	SOC/OC	SOC (μg/m^3)	SOA (μg/m^3)	SOC/OC	S OC (μg/m^3)	SOA (μg/m^3)	SOC/OC	SOC (μg/m^3)	SOA (μg/m^3)	SOC/OC	SOC (μg/m^3)	SOA (μg/m^3)	SOC/OC
Winter	7.5 ± 4.2	15 ± 8.4	0.3 ± 0.1	14.8 ± 9.1	29.6 ± 18.2	0.4 ± 0.2	8.2 ± 6.3	16.3 ± 12.6	0.3 ± 0.1	10.5 ± 7.3	20.9 ± 14.7	0.4 ± 0.1	16.4 ± 9.9	32.8 ± 19.8	0.5 ± 0.1
Summer	2.1 ± 2.0	4.2 ± 3.9	0.3 ± 0.2	3.9 ± 2.0	7.8 ± 4.0	0.4 ± 0.2	1.9 ± 1.5	3.7 ± 2.9	0.2 ± 0.1	3.4 ± 3.9	6.8 ± 7.8	0.3 ± 0.2	2.6 ± 1.4	5.2 ± 2.7	0.3 ± 0.1
Monsoon	1.5 ± 1.0	3 ± 2.1	0.3 ± 0.1	3.2 ± 1.9	6.3 ± 3.8	0.4 ± 0.2	1.9 ± 1.5	3.9 ± 3.0	0.3 ± 0.2	2.1 ± 1.6	4.2 ± 3.1	0.4 ± 0.2	1.8 ± 1.3	3.7 ± 2.7	0.4 ± 0.1
Post-monsoon	21.4 ± 13.3	42.7 ± 26.1	0.5 ± 0.2	27.9 ± 12.9	55.7 ± 25.8	0.6 ± 0.1	33.0 ± 28.0	66.0 ± 56.0	0.6 ± 0.3	19.5 ± 12.1	39.0 ± 24.2	0.6 ± 0.2	17.1 ± 16.1	34.1 ± 32.2	0.4 ± 0.3

to 6.8 (avg: 3.3 ± 1.5). Rengarajan et al. (2007) also observed a range of 3.6 ± 2.4 in Hisar. The ratios varied from 0.01 to 12.16 (avg: 2.7 ± 1.8) at IITD, 0.5 to 25.5 (avg: 2.9 ± 3) at IITMD, 0.5 to 5.9 (avg: 2.5 ± 1.1) at MRIIRS and 0.7 to 13 (avg: 2.9 ± 1.8) at IITK suggesting the contribution from mixed sources (Srinivas and Sarin, 2014). Calcium (Ca) is soluble in water and can be used as an indicator of mineral aerosols (Rastogi and Sarin, 2006). The concentration of Ca^{2+} in $PM_{2.5}$ aerosols was found to be higher in the summer than in the post-monsoon and winter at all the sites. This is prominent from the low total carbonaceous aerosols (TCA) to Ca^{2+} ratio in the summer (Hisar~12 ± 6, IITD~15 ± 5, IITMD~9 ± 2, MRIIRS~18 ± 8, and IITK~27 ± 8) compared to relatively higher ratio during the winter (Hisar~92 ± 28, IITD~82 ± 30, IITMD~97 ± 29, MRIIRS~68 ± 22, and IITK~95 ± 31). TCA can be estimated by adding the mass concentrations of organic matter (OM) and EC, whereas OM content can be computed based on organic carbon measured in the $PM_{2.5}$ aerosols (i.e., OM = 2.0 × OC). The organic (also referred as OM) and inorganic concentrations were measured by deploying Aerodyne Aerosol Mass Spectrometer (AMS) at IITMD and MRIIRS sites during Jan-March, 2018 (Lalchandani et al. manuscript under review). The calculated OM/OC ratio was observed to be in the range of ~1.52–2.3 (2.0 ± 0.19). Therefore, we have used OM/OC of 2 in our study. However, other values for OM/OC ratios (1.2–2.1) have been reported in the literature (Turpin and Lim, 2001), a ratio of 1.6 has been adopted for urban aerosols in Rengarajan et al. (2007).

3.3. Mass concentration of WSOC and WSOC/OC ratio

Water-soluble secondary aerosol fraction plays a vital role in forming cloud condensation nuclei (CCN) and fog. A large temporal variability was noticed in WSOC/OC ratios during the entire sampling period. The WSOC/OC varied annually from 0.5 to 0.9 at all the sites. The average WSOC/OC ratios were relatively higher in the samples collected during summer and monsoon compared to winter and post-monsoon at all the sites except Hisar (Fig. 7). The seasonal average WSOC/OC ratios varied from 0.8 ± 0.1 during summer and monsoon in all the sites except IITK (0.9 ± 0.1). The fractions were lower during post-monsoon (0.6 ± 0.1 in Hisar, IITD and MRIIRS, 0.7 ± 0.1 in IITMD and 0.8 ± 0.1 in IITK). In winter, the WSOC/OC ratios were 0.7 ± 0.1 in IITD, IITMD and MRIIRS, 0.8 ± 0.1 in IITK, but it was higher in Hisar~ 0.9 ± 0.1. Relatively higher WSOC/OC ratios during summer indicate contribution from photochemically derived SOA and/or aging of the aerosols during transport (Casimiro A. Pio et al., 2007). Past studies have shown lower WSOC/OC for vehicular emissions than biomass burning because of the less solubility of the organic constituents generating from the combustion of liquid fuels (diesel gasoline) (e.g., Daellenbach et al. 2016; Ram et al., 2012). A WSOC/OC ratio of 0.4 and 0.27 have been reported by Saarikoski et al. (2008) for biomass burning and vehicular emissions respectively, whereas in Daellenbach et al. (2016), it is 0.1 for traffic, 0.7 for biomass burning and 0.9 for oxidized organic aerosol, interpreted to be mostly secondary organics. Cheung et al., 2009 suggested that WSOC/OC ratios vary from 0.06 to 0.19 in the liquid fuel particles emitted from light-duty vehicles. Further, WSOC/OC ratios were higher during the day compared to night, indicating higher contribution from secondary organic aerosol (SOA) due to an increase in photochemical activity during daytime (Weber et al., 2007). The mass concentration of WSOC is largely attributed to the oxidation of volatile organic compounds (VOCs) by strong oxidants like ozone and peroxide radicals through the gas phase conversion and SOA formation (Weber et al., 2007). The seasonal and wintertime day-night values of WSOC and WSOC/OC ratios are presented in Table 3.

A value of 0.3 ± 0.1 was reported for a period during December 2004 in Hisar (Rengarajan et al., 2007), which is quite lower than our findings. Higher WSOC/OC ratios (0.3–0.8) were found during the peak of biomass burning season in the Indo-Gangetic Plain (IGP) region (Ram and Sarin, 2010). A linear relationship was observed between WSOC and OC during the sampling period at all the sites (Fig. 8). Ram and Sarin

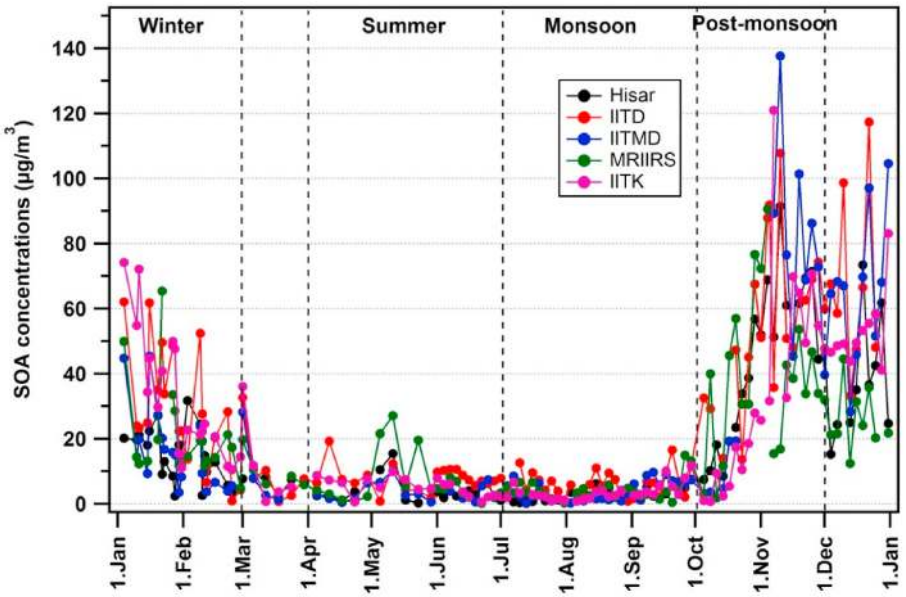

Fig. 9. Seasonal variation of SOA at the sampling sites during Jan–Dec 2018

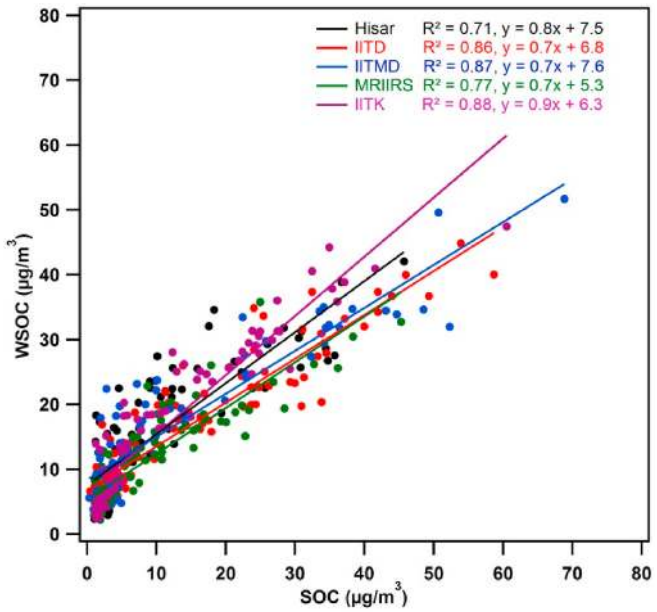

Fig. 10. Scatter plot between WSOC and SOC at the sampling sites during Jan-Dec 2018

(2010) reported that during post-monsoon higher WSOC/OC ratio indicates more SOA formation which considered the fact that SOA is water-soluble.

3.4. Estimation of SOA

Secondary organic aerosols (SOA) are formed through the gas to particle conversion of photo-oxidized products of biogenic or anthropogenic volatile organic compounds (VOCs) (Hallquist et al., 2009). SOA can be estimated through an indirect method known as the EC-tracer method (Turpin et al., 1991) using the primary nature of EC. The method is based on the fact that EC can be used as a tracer for biogenic or anthropogenic primary organic carbon (POC) as EC is derived from primary emissions (e.g., during combustion process in high temperature) and mostly inert in nature. Therefore, the secondary organic carbon $[OC]_s$ in $PM_{2.5}$ is estimated, assuming primary OC $[OC]_p$ can be defined by,

$$[OC]_p = [OC/EC]_p \text{ x } [EC] + b$$

And the contribution of $[OC]_s$ can be defined by-

$$[OC]_s = [OC] - [OC]_p$$

Where 'b' is the contribution of the non-combustion to $[OC]_p$ (Strader et al., 1999) and it is the intercept in the EC and OC scatter plot. Contribution of biogenic sources to $[OC]_p$ is relatively small (Lim and Turpin, 2002a) and can be neglected in the estimation of primary OC. SOA and POA quantification by this method highly depends on the primary [OC/EC] ratio. However, using $[OC/EC]_p$ for calculating secondary OC leads to large uncertainties due to different primary anthropogenic sources that include biomass burning emissions, fossil-fuel combustion, etc. Therefore, several studies suggested different techniques to estimate the primary [OC/EC] ratio. Cabada et al. (2002) suggested to take the [OC/EC] ratio of the prevalent emission sources like vehicular emissions as the primary [OC/EC] ratio, as from vehicular emissions most of the OC and EC percentage are primary. Castro et al. (1999) suggested a simple way to get the primary [OC/EC] ratio is to take the minimum [OC/EC] ratio of the whole data set that can serve as a first order approach to calculate secondary OC, whereas Na et al. (2004) suggested to take the average of three lowest [OC/EC] ratio of the data set. Also, the OC and EC mass concentrations during low photochemical activity and peak time of high primary emissions (morning and evening period) can be used to estimate the primary [OC/EC] ratio (Turpin and Huntzicker, 1995), although there is always contamination from the freshly produced SOA. In this study, we incorporated the approach from Pio et al. (2011) to calculate secondary OC. The primary [OC/EC] ratio was estimated from the linear regression on a portion (~15%) of the seasonal data set, which contained the lowest [OC/EC] ratios. Different

seasonal primary [OC/EC] ratio was estimated for all the five sites. The small intercept (b) was observed at IITD and IITMD, which is mainly primary OC emitting from biogenic or other non-combustible sources not containing EC. The intercept (b) is relatively very small and not accounted for in the estimation of the primary OC. The correlation between OC and EC on the ~15% portion of the seasonal data set was better during summer and monsoon (R^2~0:62–0.87) than that during winter and post-monsoon (R^2~0:25–0.60) at all sites, whereas the slope (OC/EC ratio) was higher during winter and post-monsoon (Table 4.). This weak correlation and high [OC/EC] ratio during winter and post-monsoon may attribute to SOC formation or different significant primary organic carbon sources or due to the influence of highly contaminated long-range transported aerosol in sampling sites having lower fresh emissions of primary organic carbon (Na et al., 2004). However, when open biomass burning prevails in winter and post-monsoon, the EC-tracer method could possibly result in overestimation in SOC by accounting part of primary OC from biomass burning as SOC (Ding et al., 2012; Feng et al., 2013; Sudheer et al., 2015). In this study the $[OC/EC]_p$ ratios (~2.7–3.49) obtained using Pio et al. (2011) during winter at all the sites are relatively lesser than the $[OC/EC]_p$ ratio of 4.7 which was used for SOC calculation at Ahmedabad, India during winter in Rengarajan et al. (2011).

Secondary OC is multiplied by a constant to get SOA mass concentration. In this study, a value of ~2 (Lalchandani et al. manuscript under review) is used based on the AMS derived average OM/OC ratio (2.0 ± 0.19). The constant accounts for H, O, N, S atoms in the organic molecules.

SOA varied largely over one year of sampling period at all the sites. It varied annually from 0.3 to 91.4 μg/m^3 at Hisar, 0.7–117.4 μg/m^3 at IITD, 0.2–137.7 μg/m μg/m^3 at IITMD, 0.3–90.6 μg/m^3 at MRIIRS and, 0.2–120.9 μg/m^3 at Kanpur. Interestingly, it is also observed that SOA was more in winter compared to summer at all the sites. The annual average values of SOC were 36% of OC at Hisar and IITMD, 47% of OC at IITD and 43% of OC at MRIIRS and IITK. Studies in other urban areas using EC tracer method also showed that SOC fraction represents ~30%–65% of total OC (Mancilla et al., 2015; Monteiro dos Santos et al., 2016; X. Y. Zhang et al., 2012). The seasonal average values of SOC, SOA and SOC as fraction of OC is tabulated in Table 5.

We noticed a significant increase in SOA mass concentration during winter and post-monsoon (Fig. 9). Higher SOA in winter is probably due to lower mixing layer height and increased fraction of condensable secondary species due to lower atmospheric temperature (Gray et al., 1986). Other processes such as increased nucleation and condensation, as well as presence of other oxidants such as NO_3^-, Cl^- and O_3, also contribute to the SOA formation. Many studies found that SOA is mostly water-soluble (Weber et al., 2007). SOC and WSOC exhibit a linear relationship (Fig. 10) in all sites and their variability during the entire sampling period suggests a significant contribution of SOA to WSOC. SOA is likely to be water-soluble, because of the formed polar functional groups by oxidation process of VOCs (Saxena and Hildemann, 1996) and hence WSOC can be considered as a reasonable proxy for SOA (Weber et al., 2007). The very high slopes may indicate large uncertainties in the SOC determination approach. Biomass burning OC (BBOC) could also significantly contribute to WSOC. The WSOC/SOC ratios were different for different seasons and differed in the sampling sites as well. This indicates the solubility characteristics of SOC were different during winter and summer. A paired *t*-test was done on the hypothesis that the WSOC is equal at all these five sites. A significant p-value ($p < 0.05$) has been observed for Hisar, IITD, IITMD, MRIIRS, and IITK. These results showed that much of the WSOC has a regional characteristic; it is not directly emitted by vehicles and is most likely secondary in nature.

3.5. Effect of long-range transport

The three days back trajectories were computed for 500 m above ground level (AGL) for specific sampling days during winter, summer, monsoon and post-monsoon season to track the origin of the air parcel transported at the sampling site. Different dates for different site and different season were chosen based on the peak periods during winter and post-monsoon and lowest concentration during summer and monsoon, to monitor localized as well as long-range transport of aerosols. The air mass trajectories were obtained from the final run data archive of Global Data Assimilation System (GDAS) model using NOAA's (National Oceanic and Atmospheric Administration) HYSPLIT (Hybrid Single Particle Lagrangian Integrated Trajectory model) back trajectory model. As the three-sampling location IITD, IITMD, and MRIIRS are located within 1° × 1° grid, we calculated air mass back trajectories arriving at IITD only. The sites were chosen in a way that from Hisar to IITK, the sites align in the prevailing wind direction and showed calculated back trajectories for mainly three locations ~ one in upwind, i.e. Hisar, one in the downwind, i.e. IITK and, one in IITD focusing on the NCR region. The long-range transport of mineral dust originating from the cross-country borders (Iran, Afghanistan, Pakistan), and the Thar Desert caused dust storms at IGP during summer months, whereas during winter and post-monsoon the trajectories were local to regional and indicated the dominance of anthropogenic emission sources. During the peak time of agricultural waste burning (mid-Oct to mid-Nov), air mass back trajectories were more prominently from north to northwest direction, and IITD, IITK is surely affected by the emissions coming from Hisar. The air mass back trajectories, presented in Figs. S5–S7 (See Supplementary Material) are representative of the seasonal feature and manifestation of the origin of the emission sources.

4. Conclusion

This study presents year-long chemical characterization of the $PM_{2.5}$ carbonaceous aerosol fraction from 5 different sites over IGP. During winter and post-monsoon, OC was 4–5 times higher than summer and monsoon due to the shallow boundary layer and dominance of biomass burning (wood as fuel, agricultural waste), whereas the change in EC was not statistically significant ($p > 0.05$). However, a small decrease in EC, as well as OC mass concentration was noticed during monsoon at all the sites. OC/EC ratios were higher during winter (7–12) compared to summer (3–5) and even increased during post-monsoon season. Also, during winter nights OC/EC ratios were higher at all the sites except at Hisar due to active open burning and heavy-duty vehicle movement close to the sampling sites. However, no statistically significant differences (p value > 0.05) were observed at Hisar. OC as a fraction of TC during winter and summer at the sampling sites were not statistically different ($p > 0.05$), on an average OC was 80–95% of total carbon (TC) during winter and slightly decreased during summer by 65–80%. WSOC/OC ratios showed an increasing trend during summer (75–85% of OC) at all the sites in IGP except at Hisar, which provides significant evidence for secondary organic aerosol (SOA) formation. The scatter plots between WSOC and SOC at five sites and paired *t*-test results indicate that a large fraction of WSOC is of secondary origin and regional in nature. High OC/EC ratio, along with high OC/K^+ ratio, suggested that the emissions were highly dominated by biomass burning during

winter and post-monsoon. A moderate to high correlation (0.5–0.6) was observed between OC and EC at Hisar, MRIIRS, and IITK, whereas the correlation was very low (~0.3) at IITD and IITMD suggesting EC and OC sources are more different at the latter sites. SOC contributed 30–40% of OC during winter and remained same in summer and monsoon across all the sites in IGP except at IITK, whereas during post-monsoon, it increased to 40–60%. IITMD has the highest SOA contribution (~138 μg/m^3) during post-monsoon among all the sites followed by IITK, IITD, Hisar and MRIIRS. The observations reported here have implication in understanding the spatio-temporal variation in the carbonaceous aerosol and gives a brief overview of the dominant sources; more comprehensive analysis is needed to improve our understanding of the sources, their emission characteristics and potential influence on local and regional air quality.

Author contributions

HSB performed the offline analysis and data processing and wrote the manuscript. SN carried out the water-soluble inorganic ions analysis and data processing. DB assisted in the interpretation of the results and reviewing. ASHP, SNT, and NR were involved with the supervision and conceptualization. All co-authors contributed to the paper discussion and revision.

Declaration of competing interest

The authors declare that they have no known competing financial interests or personal relationships that could have appeared to influence the work reported in this paper.

Acknowledgements

The authors are thankful to R.V Satish Kumar, Vipul Lalchandani, Suneeti Mishra, Navneeth Thamban, Ashutosh Shukla and Pawan Vats for the sampling and collection of the filters in the sampling sites, Kuldeep Dixit for helping in HYSPLIT, Vaibhav Shrivastava, Amit Viswakarma and Harishankar for assisting in laboratory work. This work is financially supported by the Department of Biotechnology, Government of India (Grant No. BT/IN/UK/APHH/41/KB/2016–17) and Central Pollution Control Board (CPCB), Government of India to conduct this research under grant no. AQM/Source apportionment_EPC Project/2017. Moreover, the authors gratefully acknowledge the NOAA ARL for the provision of the HYSPLIT transport and dispersion model (http://www.arl.noaa.gov/ready.php) used in this paper.

Appendix A. Supplementary data

Supplementary data to this article can be found online at https://doi.org/10.1016/j.apr.2020.09.019.

References

Andreae, M.O., Merlet, P., 2001. Emission of trace gases and aerosols from biomass burning. Glob. Biogeochem Cycles 15 (4), 955–966.

Bautista, A.T., Pabroa, P.C.B., Santos, F.L., Quirit, L.L., Asis, J.L.B., Dy, M.A.K., Martinez, J.P.G., 2015. Intercomparison between NIOSH, IMPROVE_A, and EUSAAR_2 protocols: finding an optimal thermal-optical protocol for Philippines OC/EC samples. Atmos. Pollut. Res. 6 (2), 334–342. https://doi.org/10.5094/APR.2015.037.

Cabada, J.C., Pandis, S.N., Robinson, A.L., 2002. Sources of atmospheric carbonaceous particulate matter in pittsburgh, Pennsylvania. J. Air Waste Manag. Assoc. 52 (6), 732–741. https://doi.org/10.1080/10473289.2002.10470811.

Castro, L.M., Pio, C.A., Harrison, R.M., Smith, D.J.T., 1999. Carbonaceous aerosol in urban and rural European atmospheres: estimation of secondary organic carbon concentrations. Atmos. Environ. 33 (17), 2771–2781. https://doi.org/10.1016/S1352-2310(98)00331-8.

Cavalli, F., Putaud, J.P., 2008. Toward a standardized thermal-optical protocol for measuring atmospheric organic and elemental carbon: the eusaar protocol. ACS, Division of Environmental Chemistry - Preprints of Extended Abstracts 48 (1), 443–446. https://doi.org/10.5194/amtd-2-2321-2009.

Chen, P., Kang, S., Li, C., Zhang, Q., Guo, J., Tripathee, L., Zhang, Y., Li, G., Gul, C., Cong, Z., Wan, X., Niu, H., Panday, A.K., Rupakheti, M., Ji, Z., 2019. Carbonaceous aerosol characteristics on the Third Pole: a primary study based on the Atmospheric Pollution and Cryospheric Change (APCC) network. Environ. Pollut. 253, 49–60. https://doi.org/10.1016/j.envpol.2019.06.112.

Chester, R., 1990. Marine Geochemistry. Cambridge University Press, London, p. 698.

Cheung, KL, Polidori A, Ntziachristos L, Tzamkiozis T, Samaras Z, Cassee FR, Gerlofs M, Sioutas C, 2009. Chemical characteristics and oxidative potential of particulate matter emissions from gasoline, diesel, and biodiesel cars. Environ Sci Technol 43 (16), 6334–6340.

Chow, J.C., Watson, J.G., Chen, L.W.A., Arnott, W.P., Moosmüller, H., Fung, K., 2004. Equivalence of elemental carbon by thermal/optical reflectance and transmittance with different temperature protocols. Environ. Sci. Technol. 38 (16), 4414–4422. https://doi.org/10.1021/es034936u.

Chowdhury, S., Dey, S., Di Girolamo, L., Smith, K.R., Pillarisetti, A., Lyapustin, A., 2019. Tracking ambient PM2.5 build-up in Delhi national capital region during the dry season over 15 years using a high-resolution (1 km) satellite aerosol dataset. Atmos. Environ. 204 (February), 142–150. https://doi.org/10.1016/j.atmosenv.2019.02.029.

Daellenbach, K.R., Bozzetti, C., Křepelová, A., Canonaco, F., Wolf, R., Zotter, P., Fermo, P., Crippa, M., Slowik, J.G., Sosedova, Y., Zhang, Y., Huang, R.J., Poulain, L., Szidat, S., Baltensperger, U., I, Haddad, El, Prévôt, A.S.H., 2016. Characterization and source apportionment of organic aerosol using offline aerosol mass spectrometry. Atmos. Meas. Tech. 9 (1), 23–39.

Dey, S., Tripathi, S.N., Singh, R.P., Holben, B.N., 2005. Seasonal variability of the aerosol parameters over Kanpur, an urban site in Indo-Gangetic basin. Adv. Space Res. 36 (5), 778–782. https://doi.org/10.1016/j.asr.2005.06.040.

Ding, X., Wang, X.M., Gao, B., Fu, X.X., He, Q.F., Zhao, X.Y., Yu, J.Z., Zheng, M., 2012. Tracer-based estimation of secondary organic carbon in the Pearl River Delta, south China. J. Geophys. Res. 117, D05313. https://doi.org/10.1029/2011jd016596.

Dockery, D.W., 2001. Epidemiologic evidence of cardiovascular effects of particulate air pollution. Environ. Health Perspect. 109 (Suppl. 4), 483–486. https://doi.org/10.2307/3454657.

Duvall, R.M., Majestic, B.J., Shafer, M.M., Chuang, P.Y., Simoneit, B.R.T., Schauer, J.J., 2008. The WaterSoluble fraction of carbon, sulfur, and crustal elements in asian aerosols and asian soils. Atmos. Environ. 42, 5872–5884.

Feng, J.L., Li, M., Zhang, P., Gong, S.Y., Zhong, M., Wu, M.H., Zheng, M., Chen, C.H., Wang, H.L., Lou, S.R., 2013. Investigation of the sources and seasonal variations of secondary organic aerosols in PM2:5 in Shanghai with organic tracers. Atmos. Environ. 79, 614–622.

Fuzzi, S., Andreae, M.O., Huebert, B.J., Kulmala, M., Bond, T.C., Boy, M., Doherty, S.J., Guenther, A., Kanakidou, M., Kawamura, K., Kerminen, V.M., Lohmann, U., Russell, L.M., Pöschl, U., 2006. Critical assessment of the current state of scientific knowledge, terminology, and research needs concerning the role of organic aerosols in the atmosphere, climate, and global change. Atmos. Chem. Phys. 6 (7), 2017–2038. https://doi.org/10.5194/acp-6-2017-2006.

Gray, H.A., Cass, G.R., Huntzicker, J.J., Heyerdahl, E.K., Rau, J.A., 1986. Characteristics of atmospheric organic and elemental carbon particle concentrations in los angeles. Environ. Sci. Technol. 20 (6), 580–589. https://doi.org/10.1021/es00148a006.

Hallquist, M., Wenger, J.C., Baltensperger, U., Rudich, Y., Simpson, D., Claeys, M., Dommen, J., Donahue, N.M., George, C., Goldstein, A.H., Hamilton, J.F., Herrmann, H., Hoffmann, T., Iinuma, Y., Jang, M., Jenkin, M.E., Jimenez, J.L., Kiendler-Scharr, A., Maenhaut, W., et al., 2009. The formation, properties and impact of secondary organic aerosol: current and emerging issues. Atmos. Chem. Phys. 9 (14), 5155–5236. https://doi.org/10.5194/acp-9-5155-2009.

Hopkins, R.J., Lewis, K., Desyaterik, Y., Wang, Z., Tivanski, A.V., Arnott, W.P., Laskin, A., Gilles, M.K., 2007. Correlations between optical, chemical and physical properties of biomass burn aerosols. Geophys. Res. Lett. 34 (18), 1–5. https://doi.org/10.1029/2007GL030502.

Ji, D., Gao, M., Maenhaut, W., He, J., Wu, C., Cheng, L., Gao, W., Sun, Y., Sun, J., Xin, J., Wang, L., Wang, Y., 2019. The carbonaceous aerosol levels still remain a challenge in the Beijing-Tianjin-Hebei region of China: insights from continuous high temporal resolution measurements in multiple cities. Environ. Int. 126 (February), 171–183. https://doi.org/10.1016/j.envint.2019.02.034.

Joshi, H., Naja, M., Singh, K.P., Kumar, R., Bhardwaj, P., Babu, S.S., Satheesh, S.K., Moorthy, K.K., Chandola, H.C., 2016. Investigations of aerosol black carbon from a semi-urban site in the Indo-Gangetic Plain region. Atmos. Environ. 125, 346–359. https://doi.org/10.1016/j.atmosenv.2015.04.007.

Karanasiou, A., Diapouli, E., Cavalli, F., Eleftheriadis, K., Viana, M., Alastuey, A., Querol, X., Reche, C., 2011. On the quantification of atmospheric carbonate carbon

by thermal/optical analysis protocols. Atmospheric Measurement Techniques 4 (11), 2409–2419. https://doi.org/10.5194/amt-4-2409-2011.
Keene, W.C., Pszenny, A.P., Galloway, J.N., Hawley, M.E., 1986. Sea salt corrections and interpretations of constituent ratios in marine precipitation. J. Geophys. Res. 91, 6647. https://doi.org/10.1029/JD091iD06p06647.
Lalchnadani, V., Kumar, V., Tobler, A., Navneeth, M.T., Mishra, S., Slowik, J.G., Bhattu, D., Rai, P., Satish, R., Ganguly, D., Tiwari, S., Rastogi, N., Mocnik, G., Prevot, A., Tripathi, S.N., 2020. Real-Time characterization and source apportionment of fine particulate matter in the Delhi megacity area during late winter. Sci. Total Environ. (Under review).
Lim, H.J., Turpin, B.J., 2002. Origins of primary and secondary organic aerosol in atlanta: results of time-resolved measurements during the atlanta supersite experiment. *Environ. Sci. Technol.* 36, 4489–4496.
Liu, Z., Gao, W., Yu, Y., Hu, B., Xin, J., Sun, Y., Wang, L., Wang, G., Bi, X., Zhang, G., Xu, H., Cong, Z., He, J., Xu, J., Wang, Y., 2018. Characteristics of PM2.5 mass concentrations and chemical species in urban and background areas of China: emerging results from the CARE-China network. Atmos. Chem. Phys. 18 (12), 8849–8871. https://doi.org/10.5194/acp-18-8849-2018.
Maenhaut, W., Claeys, M., 2011. EC/OC Analyses 2010–2011, Final report, Study for the Vlaamse Milieumaatschappij (VMM), afdeling Meetnetten en Onderzoek. Flemish Environment Agency. Order number: LUC/2010/EC/OC, 25 July 2011.
Mancilla, Y., Herckes, P., Fraser, M.P., Mendoza, A., 2015. Secondary organic aerosol contributions to PM2.5 in Monterrey, Mexico: temporal and seasonal variation. Atmos. Res. 153, 348–359. https://doi.org/10.1016/j.atmosres.2014.09.009.
Martins Pereira, G., Teinilä, K., Custódio, D., Gomes Santos, A., Xian, H., Hillamo, R., Alves, C.A., Bittencourt De Andrade, J., Olímpio Da Rocha, G., Kumar, P., Balasubramanian, R., De Fátima Andrade, M., Vasconcellos, P.D.C., 2017. Particulate pollutants in the Brazilian city of Saõ Paulo: 1-year investigation for the chemical composition and source apportionment. Atmos. Chem. Phys. 17 (19), 11943–11969. https://doi.org/10.5194/acp-17-11943-2017.
Menon, S., Hansen, J., Nazarenko, L., 2002. 2002_Menon_etal_2.pdf> 297 (September), 2250–2253.
Mikhailov, E.F., Mironova, S., Mironov, G., Vlasenko, S., Panov, A., Chi, X., Walter, D., Carbone, S., Artaxo, P., Heimann, M., Lavric, J., Pöschl, U., Andreae, M.O., 2017. Long-term measurements (2010-2014) of carbonaceous aerosol and carbon monoxide at the Zotino Tall Tower Observatory (ZOTTO) in central Siberia. Atmos. Chem. Phys. 17 (23), 14365–14392. https://doi.org/10.5194/acp-17-14365-2017.
Mkoma, S.L., Kawamura, K., Fu, P.Q., 2013. Contributions of biomass/biofuel burning to organic aerosols and particulate matter in Tanzania, East Africa, based on analyses of ionic species, organic and elemental carbon, levoglucosan and mannosan. Atmos. Chem. Phys. 13 (20), 10325–10338. https://doi.org/10.5194/acp-13-10325-2013.
Monteiro dos Santos, D.A., Brito, J.F., Godoy, J.M., Artaxo, P., 2016. Ambient concentrations and insights on organic and elemental carbon dynamics in São Paulo, Brazil. Atmos. Environ. 144, 226–233. https://doi.org/10.1016/j.atmosenv.2016.08.081.
Na, K., Sawant, A.A., Song, C., Cocker, D.R., 2004. Primary and secondary carbonaceous species in the atmosphere of Western Riverside County, California. Atmos. Environ. 38 (9), 1345–1355. https://doi.org/10.1016/j.atmosenv.2003.11.023.
Nair, V.S., Moorthy, K.K., Alappattu, D.P., Kunhikrishnan, P.K., George, S., Nair, P.R., Babu, S.S., Abish, B., Satheesh, S.K., Tripathi, S.N., Niranjan, K., Madhavan, B.L., Srikant, V., Dutt, C.B.S., Badarinath, K.V.S., Reddy, R.R., 2007. Wintertime aerosol characteristics over the Indo-Gangetic Plain (IGP): impacts of local boundary layer processes and long-range transport. Journal of Geophysical Research Atmospheres 112 (13), 1–15. https://doi.org/10.1029/2006JD008099.
Novakov, T., Menon, S., Kirchstetter, T.W., Koch, D., Hansen, J.E., 2005. Aerosol organic carbon to black carbon ratios: analysis of published data and implications for climate forcing. Journal of Geophysical Research Atmospheres 110 (21), 1–12. https://doi.org/10.1029/2005JD005977.
Pant, P., Shukla, A., Kohl, S.D., Chow, J.C., Watson, J.G., Harrison, R.M., 2015. Characterization of ambient PM2.5 at a pollution renghotspot in New Delhi, India and inference of sources. Atmos. Environ. 109, 178–189.
Panteliadis, P., Hafkenscheid, T., Cary, B., Diapouli, E., Fischer, A., Favez, O., Quincey, P., Viana, M., Hitzenberger, R., Vecchi, R., Saraga, D., Sciare, J., Jaffrezo, J. L., John, A., Schwarz, J., Giannoni, M., Novak, J., Karanasiou, A., Fermo, P., Maenhaut, W., 2015. ECOC comparison exercise with identical thermal protocols after temperature offset correction - instrument diagnostics by in-depth evaluation of operational parameters. Atmospheric Measurement Techniques 8 (2), 779–792. https://doi.org/10.5194/amt-8-779-2015.
Peterson, M.R., Richards, M.H., 2002. Thermal–optical transmittance analysis for organic, elemental, carbonate, total carbon, and OCX2 in PM2.5 by the EPA/NIOSH method. In: Proceedings of Symposium on Air Quality Measurement Methods and Technology. November 13–15, 2002,Pittsburgh,PA,pp.83–1–83–19.
Pio, C.A., Legrand, M., Alves, C.A., Oliveira, T., Afonso, J., Caseiro, A., Puxbaum, H., Sanchez-Ochoa, A., Gelencsér, A., 2008. Chemical composition of atmospheric aerosols during the 2003 summer intense forest fire period. Atmos. Environ. 42 (32), 7530–7543. https://doi.org/10.1016/j.atmosenv.2008.05.032.
Pio, Casimiro A., Legrand, M., Oliveira, T., Afonso, J., Santos, C., Caseiro, A., Fialho, P., Barata, F., Puxbaum, H., Sanchez-Ochoa, A., Kasper-Giebl, A., Gelencsér, A., Preunkert, S., Schock, M., 2007. Climatology of aerosol composition (organic versus inorganic) at nonurban sites on a west-east transect across Europe. Journal of Geophysical Research Atmospheres 112 (23). https://doi.org/10.1029/2006JD008038.
Pio, C., Cerqueira, M., Harrison, R.M., Nunes, T., Mirante, F., Alves, C., Oliveira, C., Sanchez de la Campa, A., Artíñano, B., Matos, M., 2011. OC/EC ratio observations in Europe: Re-thinking the approach for apportionment between primary and secondary organic carbon. Atmos. Environ. 45 (34), 6121–6132. https://doi.org/10.1016/j.atmosenv.2011.08.045.
Pósfai, M., Gelencsér, A., Simonics, R., Arató, K., Li, J., Hobbs, P.V., Buseck, P.R., 2004. Atmospheric tar balls: particles from biomass and biofuel burning. J. Geophys. Res.: Atmospheres 109 (6), 1–9. https://doi.org/10.1029/2003jd004169.
Psichoudaki, M., Pandis, S.N., 2013 Sep. Atmospheric aerosol water-soluble organic carbon measurement: a theoretical analysis. Environ. Sci. Technol. 47 (17), 9791–9798. https://doi.org/10.1021/es402270y.PMID:23883352.
Rai, P., Furger, M., El Haddad, I., Kumar, V., Wang, L., Singh, A., Dixit, K., Bhattu, D., Petit, J.-E., Ganguly, D., Rastogi, N., Baltensperger, U., Tripathi, S.N., Slowik, J.G., Prevot, A.S.H., 2020. Real-time Measurement and Source Apportionment of Elements in Delhi's Atmosphere. Science of Total Environment (in press).
Rajput, P., Sarin, M., Sharma, D., Singh, D., 2014. Characteristics and emission budget of carbonaceous species from post-harvest agricultural-waste burning in source region of the Indo-Gangetic plain. Tellus Ser. B Chem. Phys. Meteorol. 66 (1) https://doi.org/10.3402/tellusb.v66.21026.
Ram, K., Sarin, M.M., 2010. Spatio-temporal variability in atmospheric abundances of EC, OC and WSOC over Northern India. J. Aerosol Sci. 41 (1), 88–98. https://doi.org/10.1016/j.jaerosci.2009.11.004.
Ram, K., Sarin, M.M., Sudheer, A.K., Rengarajan, R., 2012. Carbonaceous and secondary inorganic aerosols during wintertime fog and haze over urban sites in the Indo-Gangetic plain. Aerosol and Air Quality Research 12 (3), 355–366. https://doi.org/10.4209/aaqr.2011.07.0105.
Ram, K., Sarin, M.M., Tripathi, S.N., 2010. A 1 year record of carbonaceous aerosols from an urban site in the Indo-Gangetic Plain: characterization, sources, and temporal variability. Journal of Geophysical Research Atmospheres 115 (24). https://doi.org/10.1029/2010JD014188.
Ramadan, Z., Song, X.H., Hopke, P.K., 2000. Identification of sources of phoenix aerosol by positive matrix factorization. J. Air Waste Manag. Assoc. 50 (8), 1308–1320. https://doi.org/10.1080/10473289.2000.10464173.
Rastogi, N, Sarin, M M, 2006. Chemistry of aerosols over a semi-arid region: Evidence for acid neutralization by mineral dust. Geophys. Res. Lett. 33, L23815 https://doi.org/10.1029/2006gl027708.
Rengarajan, R., Sarin, M.M., Sudheer, A.K., 2007. Carbonaceous and inorganic species in atmospheric aerosols during wintertime over urban and high-altitude sites in North India. Journal of Geophysical Research Atmospheres 112 (21), 1–16. https://doi.org/10.1029/2006JD008150.
Rengarajan, R., Sudheer, A.K., Sarin, M.M., 2011. Wintertime PM2.5 and PM10 carbonaceous and inorganic constituents from urban site in western India. Atmos. Res. 102 (4), 420–431. https://doi.org/10.1016/j.atmosres.2011.09.005.
Saarikoski, S., Timonen, H., Saarnio, K., Aurela, M., Järvi, L., Keronen, P., Kerminen, V. M., Hillamo, R., 2008. Sources of organic carbon in fine particulate matter in northern European urban air. Atmos. Chem. Phys. 8 (20), 6281–6295. https://doi.org/10.5194/acp-8-6281-2008.
Salam, A., Bauer, H., Kassin, K., Ullah, S.M., Puxbaum, H., 2003. Aerosol chemical characteristics of a mega-city in Southeast Asia (dhaka-Bangladesh). Atmos. Environ. 37 (18), 2517–2528. https://doi.org/10.1016/S1352-2310(03)00135-3.
Sandradewi, J., Prévôt, A.S.H., Szidat, S., Perron, N., Rami Alfarra, M., Lanz, V.A., Weingartner, E., Baltensperger, U., 2008. Using aerosol light absorption measurements for the quantitative determination of wood burning and Traffic emission contributions to particulate matter. Environ. Sci. Technol. 42 (9), 3316–3323.
Saxena, P., Hildemann, L.M., 1996. Water-soluble organics in atmospheric particles: a critical review of the literature and application of thermodynamics to identify candidate compounds. J. Atmos. Chem. 24, 57–109.
Sharma, D., Kulshrestha, U.C., 2014. Spatial and temporal patterns of air pollutants in rural and urban areas of India. Environ. Pollut. 195 (2), 276–281. https://doi.org/10.1016/j.envpol.2014.08.026.
Sharma, S.K., Mandal, T.K., Saxena, M., Rashmi Sharma, A., Datta, A., Saud, T., 2014. Variation of OC, EC, WSIC and trace metals of PM10 in Delhi, India. J. Atmos. Sol. Terr. Phys. 113, 10–22. https://doi.org/10.1016/j.jastp.2014.02.008.
Singh, R.P., Dey, S., Tripathi, S.N., Tare, V., Holben, B., 2004. Variability of aerosol parameters over Kanpur, northern India. J. Geophys. Res. Atmos. 109 (23), 1–14. https://doi.org/10.1029/2004JD004966.
Srinivas, B., Sarin, M.M., 2014. PM2.5, EC and OC in atmospheric outflow from the Indo-Gangetic Plain: temporal variability and aerosol organic carbon-to-organic mass conversion factor. Sci. Total Environ. 487 (1), 196–205. https://doi.org/10.1016/j.scitotenv.2014.04.002.
Srivastava, A.K., Bisht, D.S., Ram, K., Tiwari, S., Srivastava, M.K., 2014. Characterization of carbonaceous aerosols over Delhi in Ganga basin: seasonal variability and possible sources. Environ. Sci. Pollut. Control Ser. 21 (14), 8610–8619. https://doi.org/10.1007/s11356-014-2660-y.
Strader, R., Lurmann, F., Pandis, S., 1999. Evaluation of secondary organic aerosol formation in winter. Atmos. Environ 33, 4849–4863.
Sudheer, A.K., Rengarajan, R., Sheel, V., 2015. Secondary organic aerosol over an urban environment in a semi–arid region of western India. Atmospheric Pollution Research 6 (1), 11–20. https://doi.org/10.5094/APR.2015.002.
Sun, Q., Hong, X., Wold, L.E., 2010. Cardiovascular effects of ambient particulate air pollution exposure. Circulation 121 (25), 2755–2765. https://doi.org/10.1161/CIRCULATIONAHA.109.893461.
Tang, R., Wu, Z., Li, X., Wang, Y., Shang, D., Xiao, Y., Li, M., Zeng, L., Wu, Z., Hallquist, M., Hu, M., Guo, S., 2018. Primary and secondary organic aerosols in summer 2016 in Beijing. Atmos. Chem. Phys. 18 (6), 4055–4068. https://doi.org/10.5194/acp-18-4055-2018.
The Intergovernmental Panel on Climate Change (IPCC), 2013. Fifth Assessment Report (AR5). http://www.ipcc.ch/report/ar5/wg1/.

Tiwari, S., Ranade, A., Singh, D., Pandey, A.K., 2005. Study of chemical species in rainwater at Ballia, a rural environment in eastern Uttar Pradesh, India. Indian J. Radio Space Phys. 35 (1), 35–41.

Tiwari, S., Srivastava, A.K., Bisht, D.S., Safai, P.D., Parmita, P., 2013. Assessment of carbonaceous aerosol over Delhi in the Indo- Gangetic Basin: characterization, sources and temporal variability. Nat. Hazards 65, 1745–1764.

Tobler, A., Bhattu, D., Canonaco, F., Lalchandani, V., Shukla, A., Thamban, N., Mishra, S., Srivastava, A.K., Bisht, D.S., Tiwari, S., Singh, S., Močnik, G., Baltensperger, U., Tripathi, S.N., Slowik, J.G., Prévôt, A.S.H., 2019. Chemical characterization of $PM_{2.5}$ and source apportionment of organic aerosol in New Delhi, India. Sci. Total Environ. (Under Review).

Tripathi, S.N., Dey, S., Tare, V., Satheesh, S.K., 2005. Aerosol black carbon radiative forcing at an industrial city in northern India. Geophys. Res. Lett. 32 (8), 1–4. https://doi.org/10.1029/2005GL022515.

Turpin, B.J., Huntzicker, J.J., Larson, S.M., Cass, G.R., 1991. Los angeles summer midday particulate carbon: primary and secondary aerosol. Environ. Sci. Technol. 25, 1788–1793.

Turpin, B.J., Huntzicker, J.J., 1995. Identification of secondary organic aerosol episodes and quantitation of primary and secondary organic aerosol concentrations during SCAQS. Atmos. Environ. 29, 3527–3544.

Turpin, B.J., Lim, H.J., 2001. Species contributions to pm2.5 mass concentrations: revisiting common assumptions for estimating organic mass. Aerosol. Sci. Technol. 35 (1), 602–610. https://doi.org/10.1080/02786820119445.

Viana, M., Chi, X., Maenhaut, W., Cafmeyer, J., Querol, X., Alastuey, A., Mikuška, P., Večeřa, Z., 2006. Influence of sampling artefacts on measured PM, OC, and EC levels in carbonaceous aerosols in an urban area. Aerosol. Sci. Technol. 40 (2), 107–117. https://doi.org/10.1080/02786820500484388.

Viana, M., Querol, X., Alastuey, A., Ballester, F., Llop, S., Esplugues, A., Fernández-Patier, R., García dos Santos, S., Herce, M.D., 2008. Characterising exposure to PM aerosols for an epidemiological study. Atmos. Environ. 42 (7), 1552–1568. https://doi.org/10.1016/j.atmosenv.2007.10.087.

Weber, R.J., Sullivan, A.P., Peltier, R.E., Russell, A., Yan, B., Zheng, M., de Grouw, J., Warneke, C., Brock, C., Holloway, J.S., Atlas, E.L., Edgerton, E., 2007. A study of secondary organic aerosol formation in the anthropogenic-influenced southeastern United States. Journal of Geophysical Research Atmospheres 112 (13), 1–13. https://doi.org/10.1029/2007JD008408.

Yao, X.H., Chan, C.K., Fang, M., Cadle, S., Chan, T., Mulawa, P., He, K.B., Ye, B.M., 2002. The water-soluble ionic composition of PM2.5 in shanghai and Beijing, China. Atmos. Environ 36, 4223–4234.

Zhang, L. wen, Chen, X., Xue, X. dan, Sun, M., Han, B., Li, C. ping, Ma, J., Yu, H., Sun, Z., Zhao, rong, jun Zhao, L., xin Liu, B., min, Y., Chen, J., Wang, P.P., Bai, Z. peng, Tang, N. jun, 2014. Long-term exposure to high particulate matter pollution and cardiovascular mortality: a 12-year cohort study in four cities in northern China. Environ. Int. 62, 41–47. https://doi.org/10.1016/j.envint.2013.09.012.

Zhang, X.Y., Wang, Y.Q., Niu, T., Zhang, X.C., Gong, S.L., Zhang, Y.M., Sun, J.Y., 2012. Atmospheric aerosol compositions in China: spatial/temporal variability, chemical signature, regional haze distribution and comparisons with global aerosols. Atmos. Chem. Phys. 12 (2), 779–799. https://doi.org/10.5194/acp-12-779-2012.

Zhang, R., Jing, J., Tao, J., Hsu, S.C., Wang, G., Cao, J., Lee, C.S.L., Zhu, L., Chen, Z., Zhao, Y., Shen, Z., 2013. Chemical characterization and source apportionment of PM2.5 in Beijing: seasonal perspective. Atmos. Chem. Phys. 13 (14), 7053–7074. https://doi.org/10.5194/acp-13-7053-2013.